Final Draft
of the original manuscript:

Controlling Actuation Performance in Physically Cross-linked Polylactone Blends Using Polylactide Stereocomplexation

Victor Izraylit[1,2], Oliver E. C. Gould[1], Tobias Rudolph[1], Karl Kratz[1], Andreas Lendlein[1,2,3]*

1 Institute of Biomaterial Science and Berlin-Brandenburg Centre for Regenerative Therapies, Helmholtz-Zentrum Geesthacht, Kantstr. 14513 Teltow, Germany

2 Institute of Chemistry, University of Potsdam, Karl-Liebknecht-Str. 24/25, 14476 Potsdam, Germany

3 Institute of Chemistry and Biochemistry, Freie Universität Berlin, Takustr. 3, 14195 Berlin, Germany

Abstract

Within the field of shape-changing materials, synthetic chemical modification has been widely used to introduce key structural units and subsequently expand the mechanical functionality of actuator devices. The introduction of architectural elements which facilitate *in-situ* control over mechanical properties and complete geometric reconfiguration of a device, are highly desirable to increase the morphological diversity of polymeric actuator materials. The subject of the present study is a multiblock copolymer with semicrystalline poly(*L*-lactide) and poly(*ε*-caprolactone)

(PLLA-PCL) segments. By harnessing the stereocomplexation of copolymer chains with a poly(*D*-lactide) oligomer (PDLA), we provide anchoring points for physical network formation, and demonstrate how a blending process can be used to efficiently vary the mechanical properties of a shape-memory actuator. We investigate the effect of molecular structure on the actuation performance of the material in cyclic thermomechanical tests, with a maximum reversible shape change $\varepsilon_{rev}' = 13.4 \pm 1.5\%$ measured at 3.1 wt.% of polylactide stereocomplex content in the multiblock copolymer matrix. The thermophysical properties, crystalline structure and phase morphology were analyzed by DSC, WAXS and AFM respectively, elucidating the structure-to-function relationship in physically cross-linked blended materials. The work demonstrates a one-step technique for manufacturing a polymeric actuator and tuning its performance *in-situ*. This approach should greatly improve the efficiency of physically cross-linked actuator fabrication, allowing composition and physical behavior to be precisely and easily controlled.

Keywords:

Multiblock copolymer, shape-memory effect, soft actuators, physical cross-linking, crystallization

Introduction

Polymeric actuator materials are capable of reversibly and repetitively changing their shape in response to an external stimulus. Their actuation behavior can be derived from a wide variety of physical phenomenons, including the swelling/deswelling of hydrogels,[1-3] self-organization of liquid crystallites,[4-6] and oriented crystallization and melting of programmable shape-memory polymers. The nature of the shape transformation can be controlled, and tailored to a specific

function, by altering the physical manifestation of the material or by modifying the macromolecular architecture of key structural components.

A shape-memory polymeric material, capable of free-standing thermoreversible motions, typically consists of three functional elements (i) actuation units, which undergo oriented crystallization during cooling and melting upon heating, (ii) skeleton units, which define the programmable shape of the actuator as well as the direction of motion, and (iii) netpoints interlinking both actuation and skeleton units.[7] Soft shape-memory polymeric actuators utilizing chemical netpoints,[8-10] and physical netpoints[11-16] have been reported. While covalently cross-linked actuator materials are restricted to shape changes determined at the point of their manufacturing, the reprocessability of physically interlinked networks enables them to undergo complete geometric reconfiguration.[9] This capability for reconfiguration allows for the definition of a new actuation pattern and physical functionality.

A wide variety of intermolecular interactions has been used to generate physical crosslinks in polymeric actuator materials. In recent work, hydrogen bonding within directly synthesized poly(3S-isobutylmorpholin-2,5-dione) networks enabled the creation of stable physical netpoints within a poly(ε-caprolactone) (PCL) matrix.[15] Ionic interactions between sodium ions in a random copolymer of poly[ethylene-co-(methacrylic acid)] with 30 wt.% methacrylic acid groups neutralized with sodium, were used to create physical netpoints.[17] Finally, thermally stable PE crystals within a diblock copolymer of PE and poly(1-octene) have been successfully utilized as physical netpoints during actuation.[18]

However, in these examples the modification of material composition, and subsequent mechanical behavior, requires costly and time consuming synthetic alterations of the polymer architecture within the material. The ability to adjust the material composition in physically cross-linked materials through an *in-situ* processing method should greatly improve our ability to implement

morphological diversity in actuating devices. Controlling the cross-link density of a polymeric actuator material is crucial to both improving its actuation performance and tailoring its physical behavior to a certain application, allowing for the variation of important material characteristics like E modulus or elongation at break. In this study we demonstrate the use of a blending approach to modify the structure of a polymeric material, allowing us to imbue it with a reprogrammable actuation capacity and to efficiently control its actuation performance. By blending a material, which is incapable of actuation in its pure form, with a low molecular weight polymeric additive we are able to vary the cross-link density and tune the actuation performance by simply adjusting the composition of the blend. Here, unlike in previous work, strong physical netpoints are formed *in situ* during the actuator material processing.

To realize this, we need to design the main component of the blend in such way that all the principal components of the matrix are embedded into its structure. Advances in multiblock copolymer chemistry have made the introduction of multiple functional chemical entities into one macromolecule possible. The potential shape-memory behavior of poly(ε-caprolactone) (PCL) has been widely demonstrated, where the polymer's broad melting transition can be used to provide both skeleton and actuator domains.[19, 20] Here, the PCL crystallite population can be bisected by the selection of a suitable actuation temperature, with the more thermally stable fraction providing a rigid backbone, while the less thermally stable fraction drives the actuation. The second requirement of our material is the provision of specific anchoring points for the formation of physical netpoints. To realize a two part blending method for network creation, a polymeric segment capable of forming stable physical netpoints when introduced to an additive compound is required. We have chosen polylactide (PLA) to introduce this function. When combined with a stereoisomer, polylactide stereocomplexation can be used to create thermally and mechanically stable crystallites.[21-23]

As the high molecular weight (number average molecular weight $M_n > 200$ kg·mol^{-1}) blend component we synthesized a multiblock copolymer composed of poly(ε-caprolactone) segments with an average segment length of approx. 60 repeating units and poly(L-lactide) segments with an average segment length of approx. 15 repeating units. The segment lengths of all components were designed to ensure the formation of stereocomplex crystallites without latent pure crystallization, to provide sufficient actuation force and to ensure the form stability of the material. While PLA homopolymers have been shown to undergo homocrystallization at average segment lengths of 5-7 repeating units,[24] the decreased flexibility of PLLA segments in a multiblock copolymer should increase the critical segment length for homocrystallization of PLLA.[25, 26] As a working principle for the *in situ* generation of physical netpoints, the formation of PLA stereocomplexes was realized by blending the copolymer with poly(D-lactide) (PDLA). This approach is facilitated by developments in synthetic methods to reliably produce oligomeric compounds.[27] The synthesis of PLLA-PCL with a well-defined segment structure was based on the self-polycondensation of diblock macromers.[28-30] Due to an insignificant amount of transesterification reaction, this technique allows the repetitive transfer of the segment structure of the diblock precursor to the multiblock copolymer. This enables the block length of the key structural units to be specified during the diblock synthesis, before scaling up to the high molecular weight multiblock copolymer.

To explore the influence of PLA stereocomplex content in the PLLA-PCL / PDLA blends on the thermal and mechanical properties of the materials, blend samples with varying weight content of PDLA homopolymer component were prepared. By varying the average molecular weight of the PDLA homopolymer component, we gained insight into the molecular weight range where physical network formation is possible. Molecular design and compositional variation were used to modify the phase-structure and thermal properties of the blends, with the aim of generating a physical network which enables functional physical behavior in the form of macroscale reversible

actuation. The molecular structure of the samples, determined using NMR and GPC, thermal properties, measured by DSC and DMTA, and crystalline structure, elucidated with WAXS and DSC measurements, were related to physical network formation and actuation function as measured by cyclic thermomechanical testing.
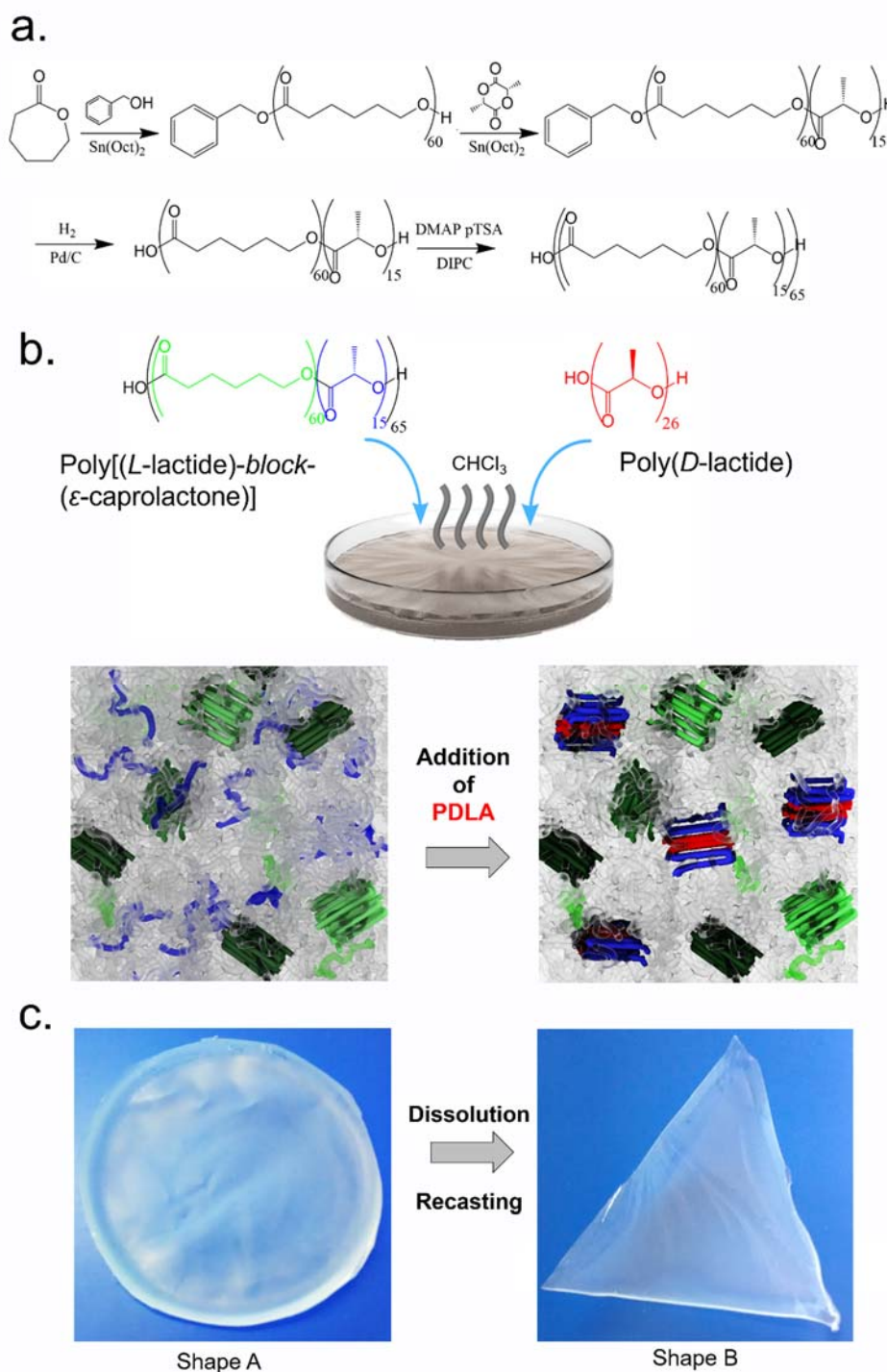
Figure 1. (a) Synthesis of multiblock copolymer containing poly(*L*-lactide) and poly(*ε*-caprolactone) segments (PLLA-PCL). Block lengths are number average values obtained from ^{1}H NMR intergration. (b) Schematic illustrating PLLA-PCL / PDLA blend structural change upon addition of PDLA homopolymer component. PDLA homopolymer (red) and PLLA segments (blue) form PLA stereocomplex crystallites, which act as physical netpoints within the polymer matrix. Crystalline PCL segments of the multiblock copolymer provide skeleton domains (dark green) and actuation domains (light green). (c) Images showing the reprocessing of the blend material via dissolution of form A in chloroform, before using solution casting to generate form B.

Experimental Section

Materials

Chloroform (99.9%, Carl Roth, Karlsruhe, Germany), toluene (99.5%, Carl Roth, Karlsruhe, Germany), methanol (99%, Carl Roth, Karlsruhe, Germany), anhydrous 1-hexanol (99%, Acros Organics, Geel, Belgium), tin(II)-2-hexanoate (Sn(Oct)$_2$) (96%, Alfa Aesar, Massachusetts, USA), dimethylaminopyridine (DMAP) (99%, Sigma-Aldrich, Missouri, USA), *p*-toluenesulfonic acid monohydrate (pTSA) (98.5%, Sigma-Aldrich, Missouri, USA), anhydrous benzylalkohol (BnOH) (98%, Acros Organics, Geel, Belgium), 10% palladium on activated carbon (Alfa Aesar, Massachusetts, USA), deuterated chloroform (99.8% Sigma-Aldrich, Missouri, USA), *L,L*-dilactide (99.5%, Corbion, Amsterdam, Netherlands) and *D,D*-dilactide (99.5%, Corbion, Amsterdam, Netherlands) were used as received. Tetrahydrofuran (THF) (99.9% Carl Roth, Karlsruhe, Germany), dichloromethane (DCM) (99.9% Carl Roth, Karlsruhe, Germany) and N,N'-diisopropylcarbodiimide (DIPC) (98%, Sigma-Aldrich, Missouri, USA) were stored over molecular sieves. *ε*-caprolactone (99%, Acros Organics, Geel, Belgium) was distilled before use. Dimethylaminopyridine p-toluenesolfonate (DMAP·pTSA) was synthesized as reported elsewhere.[31]

Nuclear magnetic resonance spectroscopy (NMR)

^{1}H NMR spectra were recorded using a DRX Avance 500 MHz spectrometer (Bruker, Rheinstetten, Germany) at room temperature in deuterated chloroform. Chemical shifts (δ) are reported in parts per million (ppm) relative to residual chloroform at δ 7.26 ppm. Samples were dissolved in CDCl$_3$ at a concentration of 15 mg·mL^{-1}. The spectra were evaluated according to the position and intensity of signals of corresponding groups.[32]

Error values for calculation of molecular weight from ^{1}H NMR data were estimated as a combination of saturation effects, intensity losses due to isotropic sidebands, unevenness of the magnetic field in the sample and the line shape causing overlapping of the peaks. An estimated error of approx. 12% of the measured value was calculated.

Gel-permeation chromatography (GPC)

Number average molecular weights of starting materials and products were determined by high-throughput gel permeation chromatography (GPC), using a Tosoh EcoSEC HLC-8320 Gel Permeation Chromatograph equipped with a refractive index detector (Tosoh Bioscience, Stuttgart, Germany) combined with a PSS Universal Data Center (PSS, Mainz, Germany), a viscometer ETA2010 (PSS, Mainz, Germany), an EcoSEC UV detector 8320 (Tosoh Bioscience), a light scattering detector SLD7100 (PSS, Mainz, Germany) and two HT-GPC columns type PSS SDV analytical linear M 5 μm (PSS, Mainz, Germany) connected in series. For the measurements, by universal calibration, tetrahydrofuran (THF) was used as an eluent (35 °C, flow rate 1.0 mL·min^{-1}) with 0.05 weight content 3,5-di-*tert*-butyl-4-hydroxytoluene as an internal standard in order to determine the hydrodynamic volume as a function of elution volume. Molecular weight and dispersity calculations were performed using WINGPC 6.2 (PSS) SEC software (Polymer

Standard Service, Mainz, Germany). The error was considered as 10% of the measured value calculated based on variations in the measurement of polystyrene calibration standards.

Differential scanning calorimetry (DSC)

DSC experiments were conducted on a Netzsch DSC 204 Phoenix (Nezsch, Selb, Germany) at heating and cooling rates of 10 K·min^{-1}. Samples were weighed directly into hermetic aluminum pans. For the determination of the thermal properties of the polymers and blends, measurements were taken during the first cooling and second heating run in the temperature range from -100 to 200 °C.

The degree of crystallinity (χ_c) of all components was calculated from the obtained melting enthalpies (ΔH_m) according to the equation:

$$\chi_c = \frac{\Delta H_m}{\Delta H_m^{100}} \cdot \frac{1}{W} \cdot 100$$

Where ΔH_m is the experimental melting enthalpy of a fraction, determined as the area under the melting peak. ΔH_m^{100} is the specific melting enthalpy of 100% crystalline polymer, which is 135 J·g^{-1} for PCL[33] and 142 J·g^{-1} for PLA stereocomplex.[34] W is the weight content of the fraction in the copolymer of the blend. The PLA stereocomplex fraction was calculated as the maximal amount of coupling *L*- and *D*-lactide units. DSC was used for the measurement of χ_c to enable the characterization of our samples at 0 °C, as opposed to at ambient temperature (25 °C) where the PCL segment of the multiblock copolymer is partially molten. A statistical error of 10% for the measured enthalpy and 1 °C for the peak position provided by the manufacturer was considered for the measurements.

Dynamic mechanical thermal analysis (DMTA)

DMTA measurements were performed using an Eplexor 25 N (Gabo, Ahlden, Germany) equipped with a 25 N load cell using a standard test specimen type (DIN EN ISO 527-2/1BB). The applied oscillation frequency was 1 Hz. The measurement was performed in the temperature sweep mode from -100 to 100 °C with a constant heating rate of 1 °C·min^{-1}. The glass transition (T_g) was determined at the peak maximum of loss modulus (E'') vs temperature curve. Temperature measurements were recorded with a manufacturer-determined accuracy of $\Delta T = 1$ °C.

Wide-angle X-ray scattering (WAXS)

WAXS measurements were performed with a D8 Discover spectrometer with a 2D-detector from Brucker AXS (Karlsruhe, Germany) in the temperature range of 25 – 100 °C. The samples of dimensions 2 x 0.5 cm and width 150 μm were fixed at both ends during characterization. Peak position was determined with $\Delta\theta = 0.1°$ error originating from variations in sample thickness and position in the sample holder.

Thermomechanical testing

All mechanical tests were performed using a thermomechanical tensile tester Zwick Z1.0 (Ulm, Germany) equipped with a thermochamber and a temperature controller. A clamping distance of 10 mm was used in all of the experiments. Elongation at break ε_{break} of the samples was tested by stretching the samples at defined temperatures and a constant deformation rate of 5 mm·min^{-1} until breakage occurred. The actuation capability of the material was characterized by programming, followed by three repetitive actuation cycles. The sample was heated in the thermo-chamber at the programming temperature $T_{prog} = 70$ °C for 10 minutes to remove the thermal history in the PCL

segments. Then, the sample was elongated to the programming strain ε_{prog} = 300% - 1250% at 5 mm·min^{-1}. The sample was held at T_{prog} and ε_{prog} for 5 min to allow the initial relaxation processes align the polymer chains along the deformation axis. At the final step of programming, the temporary shape was fixed at 0 °C under constant force. Then the force applied to the sample was reduced to 0.05 N, at which zero-force reversible shape-memory effect (rbSME) test was carried out. The actuation cycle was performed in a temperature window 0 – 55 °C, where the minimum temperature of the actuation cycle T_{low} = 0 °C was defined based on DSC data and the maximum temperature of the actuation cycle T_{high} = 55 °C was defined in a rbSME experiment where T_{high} was systematically varied. A sample was programmed at T_{prog} = 70 °C and ε_{prog} = 1000% with shape fixation at T_{low} = 0 °C. An actuation cycle was conducted between T_{low} = 0 °C and a T_{high} which was raised between 50 °C and 100 °C in 5 °C increments for each consequent cycle. The cycle with the highest ε_{rev}' was used to determine the T_{high} value used in subsequent experiments. Actuation performance ε_{rev}' was calculated as:

$$\varepsilon_{rev}' = \frac{l_b - l_a}{l_a} \cdot 100\% = \frac{\varepsilon_b - \varepsilon_a}{\varepsilon_a + 100} \cdot 100\% ,$$

where l_a and ε_a are the length of the sample and its engineering strain at the beginning of the actuation cycle at T_{high} and l_b and ε_b are the length of the sample and its engineering strain at the beginning of the actuation cycle at T_{low}. The ε_{rev}' values were calculated as an average in three subsequent cycles. The process is schematically illustrated in Figure S2.

Atomic force microscopy (AFM)

AFM measurements were performed on a MFP-3D-BioTM AFM (Asylum Research, Goleta, USA) equipped with a Cooler/Heater controller (Asylum Research, Goleta, USA). Samples were prepared by cutting with a diamond knife. The samples, with an approximate thickness of 100 nm,

were placed on a silica grid before imaging, and imaged at 28 °C and at 70 °C. Samples were equilibrated at each investigated temperature for 10 min before measurement. AC mode with a scan rate of 0.5 Hz was used for imaging. AC200TS probes (Olympus, Tokyo, Japan) with a typical driving frequency of approximately 150 kHz (individual variation from 100 to 200 kHz) and a typical spring constant of approximately $9 \, N \cdot m^{-1}$ (individual variation from 2.8 to 21 $N \cdot m^{-1}$) were used. The tip radius and height were 5–10 nm and $14 \pm 1 \, \mu m$ respectively, with a three-side shape (front angle of $0 \pm 1°$, a back angle of $35 \pm 1°$, and a side angle of $15 \pm 1°$). A scan size of 1 $\times 1 \, \mu m$ was used.

Synthesis of multiblock copolymer with poly(*L*-lactide) and poly(*ε*-caprolactone) segments (PLLA-PCL)

A PCL-precursor was synthesized via ring-opening polymerization (ROP) of *ε*-caprolactone. 100 g *ε*-caprolactone were put into closed reaction flask under an argon flow and heated to 140 °C with an oil bath. 1300 mg BnOH and 178 mg Sn(Oct)$_2$ were added through a syringe in 50 mg·ml^{-1} dry THF solutions. After 2.5 h the reaction mixture was cooled and dissolved in 500 mL chloroform. Precipitation into methanol gave a white precipitate, which was filtered through a glass filter with average pore size 10-16 μm and dried under vacuum. A yield of 94% was recorded. PLLA-PCL was synthesized via ROP of *L,L*-dilactide with PCL as the macroinitiator. Then, 31 g of PCL was dissolved in 150 mL of toluene and dried using a rotary evaporator. The PCL was then placed into a reaction flask with 10 g *L,L*-dilactide under argon flux. The vessel was then heated to 140 °C using an oil bath. A 56 mg Sn(Oct)$_2$ was added through a syringe at a concentration of 50 mg·mL^{-1} in dry THF solution. After 4 h, the reaction mixture was cooled and dissolved in 250 mL of chloroform. The reaction mixture was precipitated into methanol, resulting in a white precipitate, which was filtered through a glass filter with average pore size 10-16 μm and dried under vacuum.

An 88% conversion of *L,L*-dilactide was determined by NMR measurements. The benzyl protective group was removed via a hydrogenation reaction. A 30 g of PLLA-PCL diblock copolymer was dissolved in 150 mL of THF and put into a Büchi ecoclave reactor. Then, 300 mg Pd/C was added. The reaction was left for 36 hours at 50 °C under a hydrogen atmosphere. The reaction mixture was precipitated into methanol, and the resulting white precipitate was filtered through a glass filter with average pore size 10-16 μm and dried under vacuum. The final multiblock copolymer was synthesized via self-polycondensation reactions of the PLLA-PCL diblock copolymers. Then 4 g of the multiblock copolymer was dissolved in 100 mL toluene and dried using a rotary evaporator. The multiblock copolymer was then put into a reaction flask under argon and dissolved in DCM. Here, 8.8 g DMAP, 35.2 g DMAP·pTSA and 85 mg DIPC were added as DCM solutions. The reaction lasted 3 days at ambient temperature. The reaction mixture was diluted with 100 mL DCM and precipitated into methanol giving a white precipitate, which was filtered and dried in vacuum. The PLLA-PCL multiblock copolymer used in the study was PLLA15-PCL64, where indexes stand for the average segment length in repeating units, as determined using NMR. The molecular structure of the synthesized multiblock copolymer is presented in the Table S1. An exemplary NMR spectrum is presented in Figure S1.
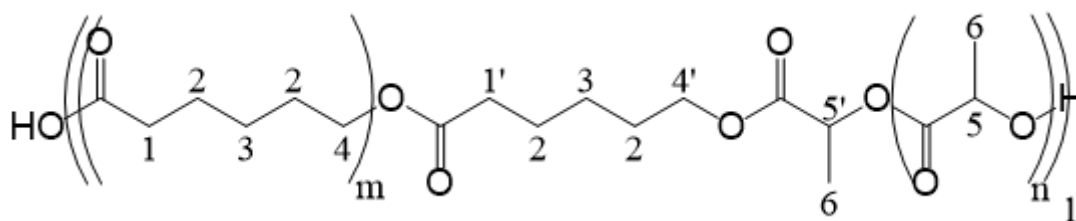
^{1}H NMR (500 MHz CDCl₃) δ = 5.15 (q, nH, CH-5); 5.1 (q, H, CH-5'); 4.15 (t, 2H, CH₂-4'); 4.05 (t, mH, CH₂-4'); 2.4 (t, 2H, CH₂-1'); 2.3 (t, mH, CH₂-1); 1.65 (m, 4(m+1)H, CH₂-2), 1.6 (d, 3(n+1)H, CH₃-6), 1.4 (m, 2(m+1)H, CH₂-3), where m+1 and n+1 are the number average segment lengths of PCL and PLLA respectively the PLLA-PCL multiblock copolymer and l is the number

average count of PLLA-PCL diblock repeating units in the multiblock copolymer. Signals of the groups marked with a prime originate from monomer (PCL or PLLA) units having an opposite neighboring monomer unit (PLLA or PCL respectively) in the multiblock copolymer chain. m was determined as the ratio of the integral intensities of δ 2.3 and δ 2.4 peaks. n was determined as δ 5.15 and δ 5.1 maxima. The molar ratio of PLLA and PCL in the block copolymers was calculated as the ratio of the integral intensities of the signals in the δ 5 – 5.2 ppm and δ 5 – 5.2 ppm regions. To calculate the number average molecular weight M_{NMR} of the diblock repeating units the ratios were then multiplied by the molecular weight M_{PLA} = 72 kg · mol^{-1} and M_{PCL} = 114 kg · mol^{-1} respectively.

PDLA was synthesized via Sn(Oct)$_2$ catalyzed 1-hexanol initiated ROP of *D,D*-dilactide. A series of PDLA samples with different molecular weight in the range M_n = 0.6 – 3.5 kg · mol^{-1} were achieved. The exemplary synthesis was performed as following: 15 g *D,D*-dilactide was transferred to a closed reaction flask under an argon flow and heated to 140 °C with an oil bath. 2.1 g 1-hexanol and 40 mg Sn(Oct)$_2$ as 50 mg·mL^{-1} dry THF solution were added through a syringe. After 45 min the reaction mixture was cooled and dissolved in 20 mL chloroform. Precipitation into cold methanol gave a white precipitate, which was filtered through a glass filter with average pore size 10-16 µm and dried under vacuum. A yield of 81% was recorded.
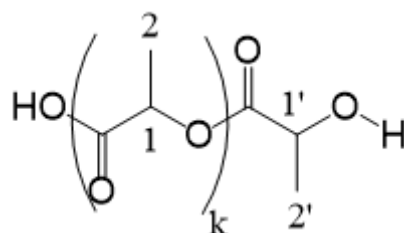
^{1}H NMR (500 MHz CDCl$_3$) δ = 5.15 (q, *k*H, CH-1); 4.35 (q, H, CH-1'); 1.6 (d, 3*k*H, CH$_3$-6), 1.4 (d, 3*k*H, CH$_3$-6'), where k+1 is the number average segment length of PDLA molecules. Signals of the groups marked with an apostrophe originate from the monomer units located in the end of

the polymer chain. k was determined as the ratio of the integral intensities of the signals in δ 5.15 and δ 4.35 regions. The number average molecular weight M_{NMR} of PDLA was calculated by multiplication of the ratio of intergral intensities by the molecular weight $M_{PLA} = 72$ kg $\cdot$ mol^{-1} of a repeating unit.

Film Preparation

Films were prepared via solution casting. The components of the blend were dissolved in a predetermined ratio in chloroform. The solution was stirred for 3 hours until the polymers were dissolved, before pouring into a PTFE Petri dish, covering with aluminum foil and left to evaporate in ambient conditions for several hours. Dog-bone-shape specimens (length 10 mm, width 3 mm, with an increased grip fixation area) were cut for mechanical testing. To reprocess a prepared sample into an alternative shape, the material was dissolved in chloroform and recast from solution into an alternative mold. Molds in the shape of a circle and triangle were used for the films prepared, shown in figure 1c.

Results and Discussion

Design, synthesis and characterization of PLLA-PCL / PDLA blends

The design of PLLA-PCL and PDLA aimed to maximize the actuation performance of the final blend material by optimizing the property-function ratio on a molecular level. As stated previously, two thermally distinct crystalline domains are required within the material for successful actuation, PCL crystallites to provide actuator and skeleton domains and PLA stereocomplex crystallites to provide the cross-links necessary to ensure the network structure. To prevent the crystallization of PLLA polymer segments before stereocomplexation, their length was reduced to an average segment length of 15 repeating units. This number was experimentally determined as the chain length of PLLA long enough for PLA stereocomplex formation, but too short for the solitary crystallization. While PLA homopolymers have been shown to undergo homocrystallization at average segment lengths of 7 repeating units,[24] the decreased flexibility of PLLA segments in a multiblock copolymer[25, 26]explains the observed lack of homocrystallization in the material. For PCL, an average block length of approx. 60 repeating units was chosen to provide a sufficient amount of actuation force during temperature change. A list of prepared samples can be found in Table S1. Further increasing the average PCL segment length lead to synthetic complications, originating from steric hindrance during knotting of the polymer chain, reducing the availability of hydroxyl groups during initiation of *L,L*-dilactide ring-opening polymerization.

GPC analysis (Figure S3) of PDLA homopolymers synthesized with lower number average chain lengths (3, 6 and 9 repeating units as measured by NMR) showed an increase in polydispersity index (Đ) from 1.17 to 1.42 with a decrease in average chain length from 26 to 3 repeating units, as shown in Table S2. This increase of Đ, and the overall decrease of molecular weight, was undesirable in this study as it increased the proportion of PDLA homopolymer below the critical average chain length for stereocomplex formation of 7 repeating units as determined in the literature.[24] DSC measurements of samples prepared from PLLA15-PCL64 and PDLA

homopolymers with average chain lengths of 3, 6 and 9 repeating units revealed a decrease in PLA stereocomplex crystallinity from 37±2% at an average chain length of 26 repeating units to 4±0.4% at an average chain length of 3 repeating units as shown in Table 1. WAXS measurements indicated stereocomplex formation at PDLA average chain lengths of 6, 9 and 26 repeating units but revealed no stereocomplex formation at a PDLA average segment length of 3 repeating units, as shown by the absence of $2\theta = 11°$ reflection attributed to the PLA stereocomplex (Figure S4). DSC measurements (Figure S5) also revealed that the decrease of the PDLA number average molecular weight M_n resulted in a reduction in the PLA stereocomplex melt transition maximum from 171±1 to 125±1 °C. Higher average chain lengths than 26 repeating units were experimentally found to reduce the miscibility of the PDLA with the copolymer, reducing the homogeneity of the stereocomplex formation, and increasing the formation of pure PLA crystallites. The high mobility of the low molecular weight PDLA component in solution encourages the formation of stereocomplex crystallites without the need for post processing, e.g. annealing. To maximise stereocomplex crystallinity and retain the high PDLA miscibility associated with low molecular weights, the molecular weight of PDLA was fixed at $M_n = 1.9$ kg $\cdot$mol^{-1} or an average chain length of 26 repeating units for the following experiments.

Table 1. Thermal properties of blend samples containing PLLA15-PCL64-SC10 multiblock copolymer and PDLA homopolymer as measured by DSC.

Average PDLA chain length (repeating units)	PCL				PLA stereocomplex			
	T_m (°C)[a]	T_c (°C)[a]	ΔH (J$\cdot$g^{-1})[b]	χ_c (%)[c]	T_m (°C)[a]	T_c (°C)[a]	ΔH (J$\cdot$g^{-1})[b]	χ_c (%)[c]
3	53±1	18±1	38±4	42±4	130±1	-	1.2±0.1	4±0.4
6	52±1	15±1	43±4	46±4	125±1	-	6±0.6	20±2
9	54±1	17±1	28±3	31±3	148±1	44±1	6.5±0.7	22±2
26	42±1	19±1	34±2	38±2	171±1	55±1	10±2	37±2

[a] Melting and crystallization temperatures determined as the maximum of the respective peaks in the second heating and the first cooling runs. [b] Intrinsic melting enthalpy was determined as the area under the melting peak in the second heating run. [b] Degree of crystallinity, as the ratio between the intrinsic melting enthalpy ΔH_m and the melting enthalpy of a 100% crystalline material ΔH_m^{100} which is 135 J$\cdot$g^{-1} for PCL[33] and 142 J$\cdot$g^{-1} for PLA stereocomplex.[34]

A targeted number average molecular weight of 200 kg·mol^{-1} was chosen for the copolymer for the following reasons: the stereocomplex, which acts as the physical cross-links of the polymer network, can be destroyed at high deformations of the material during shape-memory effect (SME) programming. While some elongation-induced crystallization is caused by this deformation, the overall loss in network anisotropy hinders the orientated crystallization needed for rbSME. However, some crystal sliding, which causes stereocomplex destruction, is an inevitable process with some stereocomplex crystallites destroyed and reformed. To reduce the effect of this process, the amount of cross-links, i.e. stereocomplex crystallites, per molecule should be increased. This reduces the chance that a certain polymer chain will lose orientational information upon the loss of cross-linking within the material. To increase the amount of stereocomplex crystals per molecule, without changing the blend composition, the chain length of the copolymer must be increased. This molecular weight increase leads to an improved deformability of the material, a higher obtainable molecular orientation, and higher ε_{rev}' values. The multiblock copolymer was produced with a block length and number average molecular weight measured as PLLA15-PCL64 $M_n = 238$ kg · mol^{-1}, as shown in table S1.

With increasing PDLA homopolymer weight content, excess material unable to form a stereocomplex generates pure PDLA crystallites, causing the appearance of additional PLA crystallinity. Decreasing the PDLA content to an equal or lower amount than the PLLA provided by the copolymer, removes the pure PDLA crystallinity. This is caused by the energetic preference for PDLA to form stereocomplex over pure crystallites.[34] The highest absolute PLA stereocomplex crystallinity was observed in the PLLA15-PCL64-SC10 sample. Samples with a lower PDLA content were investigated here to minimize any non-stereocomplex associated PLA crystallization. As a result of the low block length of the PLLA segment of the multiblock copolymer, PLLA polymer unoccupied by stereocomplexation with PDLA remained in an amorphous state in the polymer matrix.

The reprocessability of the PLLA-PCL / PDLA physically cross-linked matrix was demonstrated by recasting a film after initial shape formation. The PLA stereocomplex in the PLLA-PCL / PDLA blends were found to be soluble in chloroform, likely as a result of the low molecular weight of its constituents (an average segment length of 15 repeating units for the PLLA segments and average chain length of 26 repeating units for the PDLA oligomer). During this process, the physical network is destroyed and reformed during solvent evaporation with the complete loss of mechanical information within the material. Images of the initial shape and the recasted one are presented in the Figure 1c. The WAXS spectra and the DSC curves of the initial and the recasted material are presented in Figure S6. The cross-link density, i.e. stereocomplex crystallite content, was varied by alteration of the ratio of PLLA-PCL / PDLA in the blend. At high molecular weights ($M_n > 200$ kg mol^{-1}) chain entanglement can affect the mechanical properties of the physically cross-linked matrix. At 70 °C the PCL crystals are completely molten (Table 2, Figure 2 and Supplementary Figure 8) and the mechanical strength is derived solely from the PLA stereocomplex and chain entanglement. As expected, the mechanical strength of a sample was found to be dependent on the PLA stereocomplex content of the blend (Supplementary Figure 9), and at this temperature the pure PLLA-PCL possessed no mechanical strength. Hence, the contribution of molecular entanglement to the mechanical properties of the samples was deemed to be negligibly low.

Polylactide stereocomplex formation in PLLA-PCL / PDLA blends

Thermophysical data for the analyzed samples are shown in Table 2. The obtained DSC curves for sample PLLA15-PCL64 (Figure 2 and Supplementary Figure 8) displayed a melting transition with a maximum at 52±1 °C, attributed to PCL. This supports the assumption that the LLA segments of the PLLA-PCL copolymer (with a number average segment length of 15 repeating units) are too short to undergo isotactic crystallization. A sample from the blended material,

19

PLLA15-PCL64-SC10, displayed a melting temperature range of approx. $100 - 180$ °C with a peak maximum at $T_m = 171\pm1$ °C, attributed to PLA stereocomplex, with a melting enthalpy ΔH corresponding to a relative crystallinity of $\chi_c = 37 \pm 2\%$. The lower measured melting temperature of the PLA stereocomplex, when compared to literature data (> 200°C),[34] is likely the result of the relative short length of the PLA molecules involved in its formation. Data obtained for the sample PLLA15-PCL64-SC10, displayed a decrease in the T_m attributed to PCL crystallites to 42 ± 1 °C with a melt temperature range of approx. $38 - 58$ °C. This is likely the result of interactions between the PLA stereocomplex and PCL crystallites within PLLA-PCL. However, the material's χ_c remained at the same level of $38 \pm 2\%$, demonstrating a sufficient amount of PCL for actuation.
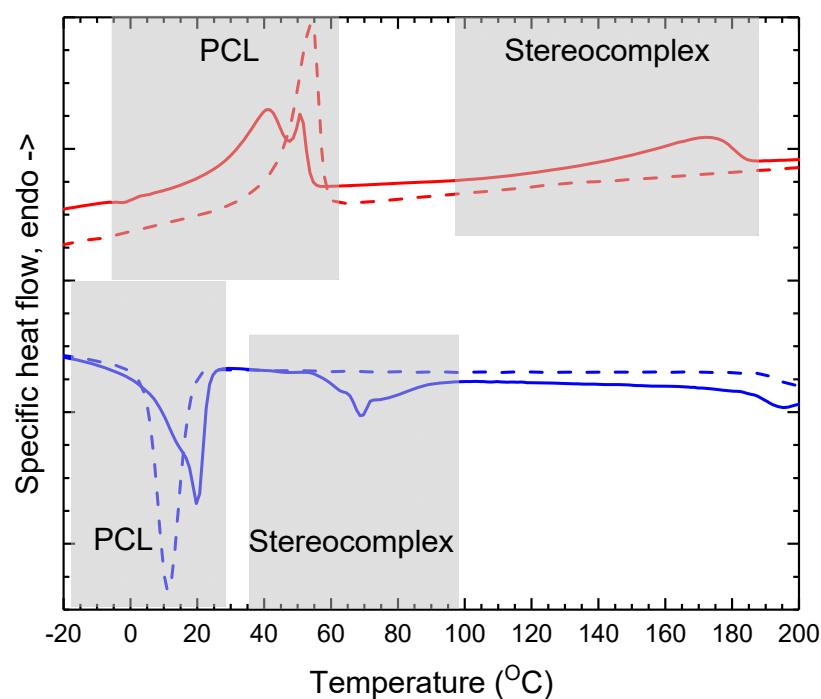

Figure 2. DSC thermograms of samples PLLA15-PCL64 (dashed line) and PLLA15-PCL64-SC10 (solid line) obtained from second heating (red) and first cooling (blue) run.

Table 2. Thermal properties of PLLA-PCL multiblock copolymer and its blends with PDLA homopolymer as measured by DSC.

Sample	PCL				PLA stereocomplex			
	$T_m{}^a$	$T_c{}^a$	ΔH^b	$\chi_c{}^c$	$T_m{}^a$	$T_c{}^a$	ΔH^b	$\chi_c{}^c$
	(°C)	(°C)	(J·g^{-1})	(%)	(°C)	(°C)	(J·g^{-1})	(%)
PLLA15-PCL64	52±1	13±1	41±4	35±4	-	-	-	-
PLLA15-PCL64-SC1	53±1	15±1	42±4	44±4	172±1	-	1±0.1	35±2
PLLA15-PCL64-SC2	51±1	16±1	47±5	48±5	171±1	51±1	1.9±0.2	28±2
PLLA15-PCL64-SC3	52±1	18±1	36±4	33±3	176±1	59±1	5.9±0.6	71±7
PLLA15-PCL64-SC4	52±1	20±1	29±3	27±3	174±1	61±1	6.5±0.7	58±6
PLLA15-PCL64-SC5	49±1	16±1	39±4	41±4	176±1	49±1	8.5±0.8	60±3
PLLA15-PCL64-SC10	43±1	20±1	37±4	41±4	178±1	78±1	15±2	56±6

[a] Melting and crystallization temperatures determined as the maximum of the respective peaks in the second heating and the first cooling runs. [b] Intrinsic melting enthalpy was determined as the area under the melting peak in the second heating run. [c] Degree of crystallinity, as the ratio between the intrinsic melting enthalpy ΔH_m and the melting enthalpy of a 100% crystalline material ΔH_m^{100} which is 135 J·g^{-1} for PCL[33] and 142 J·g^{-1} for PLA stereocomplex.[34]

WAXS was used to further elucidate the crystalline structure of the material at two temperatures: 25 °C and 70 °C. (Figure 3 and Supplementary Figure 7) At the higher temperatures the PCL is molten according to the obtained DSC data (Figure 2 and Supplementary Figure 8). Non-blended samples, such as PLLA15-PCL64, display signals attributed to PCL (110) and (200) scattering in the region $2\theta = 21.5°$ and $2\theta = 24°$ respectively. At 70 °C only an amorphous halo can be observed for this material. The measured PCL signals overlap with the scattering from PLA stereocomplex (300), (030) planes at $2\theta = 20.5°$ and (220) at $2\theta = 24°$. A free standing (110) PLA stereocomplex maximum at $2\theta = 12°$ is an indicator of its presence at 25 °C. The blend PLLA15-PCL64-SC10 retains a 12° signal at 70 °C, while the molten PCL in the other samples made identification of the signals at 20.5° and 24° difficult. Changes in the crystalline structure of the materials between 25 °C and 70 °C demonstrates that the PDLA generates a thermostable physically cross-linked matrix.
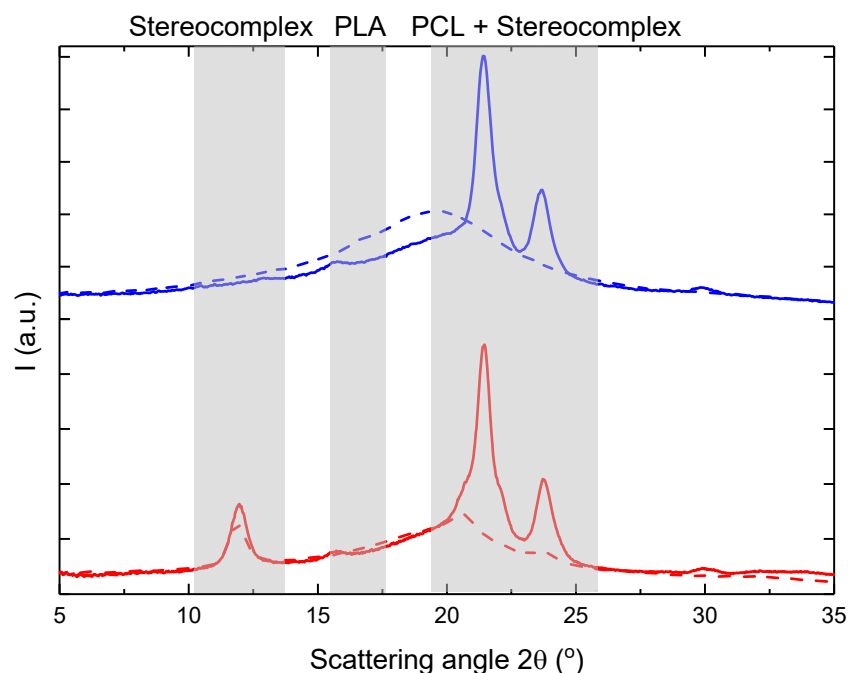
Figure 3. WAXS profiles of PLLA15-CL64 (blue) and PLLA15-CL64-SC10 (red) obtained at 25 °C (solid line) and at 70 °C (dashed line).

AFM phase images revealed the presence of hard crystalline areas at room temperature for both PLLA-PCL multiblock copolymers and its blends with 10 wt.% of PDLA (Figure S10). The blend sample displayed more hard areas than the pure PLLA-PCL, due to the presence of additional stereocomplex crystallites. Heating to 70 °C caused a complete disappearance of the hard crystals in the PLLA-PCL. In the blend sample at 70 °C, (Table 2, DSC curves are shown in Figure 2 and Supplementary Figure 8), crystallinity was observed that, due to the absence of crystalline PCL, can only originate from the PLA stereocomplex. PCL crystallinity was restored after cooling the samples to 10 °C.

Actuation capability

The rbSME performance of a material is dependent on the function of certain key structural units within the polymer matrix. Within the samples presented here, the PLA stereocomplex acts as the physical netpoints of the matrix, providing structural stability and preventing polymer slippage on deformation. By choosing a transition temperature that bisects the PCL crystallite population, it can provide both actuator and skeleton domains. The higher melting fractions stay crystallized providing the skeleton domain, and maintain network anisotropy with the polymer matrix. The PCL fractions with a lower T_m function as actuator domains, whose melting and crystallization provide the driving force for reversible macroscale shape change. The conceptual schematics of the supramolecular structure transformations during the actuation is depicted in Figure 4a.

The dependency of actuation performance on the programming strain ε_{prog} was investigated for the PLLA15-PCL64-SC1 sample using uniaxial tensile testing. The obtained results are summarized in Table 3. While an increase in the measured value of ε_{rev}' from 11% to 12.6% was observed with a decrease of ε_{prog} from 1250% to 500%, the error values obtained for these measurements (1.3 – 1.5%) prevent us from inferring a relationship between programming strain and ε_{rev}'. rbSME experiments where ε_{prog} was varied in the range of 1000 to 500% for samples PLLA15-PCL64-SC10, PLLA15-PCL64-SC2, PLLA15-PCL64-SC3, PLLA15-PCL64-SC4, PLLA15-PCL64-SC5 also showed no correlation between ε_{prog} and ε_{rev}' (Table S3). At $\varepsilon_{prog} = 300\%$ no rbSME was observed. We propose that here, the variation in deformation mechanism in different strain regions plays an important role. Literature reports have demonstrated that a semi-crystalline polymeric material undergoes structural changes upon tensile deformation in a series of different deformation modes.[35, 36] This restructuring follows different mechanisms depending on the applied strain. At the lowest elongation the deformation is purely elastic and the crystallites undergo no structural changes. Further, before the elastic limit crystalline sliding takes place in a random manner, and with increase of the strain over the elastic limit this movement becomes coordinated. An increase

in strain beyond this point causes crystalline lamellae fragmentation through fibrillation, which can be observed as strain hardening. At the highest deformation the amorphous network disentangles and the material loses any memory of the initial structure. The deformation mechanism of stereocomplex containing blends will be studied at greater length in following work. A programming strain of $\varepsilon_{prog} = 1000\%$ was chosen for further experiments.

Table 3. Measurement of ε_{rev}' in PLLA-PCL blend samples with variation of weight content of PDLA homopolymer and programming strain ε_{prog}

Sample	ε_0[a]	χ_c Stereocomplex[b]	Stereocomplex content[c]	ε_{rev}' [d]
	(%)	(%)	(wt.%)	(%)
PLLA15-PCL64-SC10	1000	37±2	7.5±0.2	5.3±0.5
PLLA15-PCL64-SC5	1000	60±3	6±0.2	7.7±0.5
PLLA15-PCL64-SC4	1000	58±6	5±0.3	10±0.7
PLLA15-PCL64-SC3	1000	71±7	3.1±0.2	13.4±1.5
PLLA15-PCL64-SC2	1000	28±2	1.1±0.1	12±1.2
PLLA15-PCL64-SC1	1250	35±2	0.7±0.1	11±1.5
PLLA15-PCL64-SC1	1000	35±2	0.7±0.1	11.4±1.5
PLLA15-PCL64-SC1	750	35±2	0.7±0.1	11.8±1.3
PLLA15-PCL64-SC1	500	35±2	0.7±0.1	12.6±1.5

[a] Programming elongation used for shape-memory experiments. [b] Degree of crystallinity of PLA stereocomplex determined with DSC as a ratio of melting enthalpy of PLA stereocomplex (integral intensity of the melting peak) to the melting enthalpy of 100% crystalline PLA stereocomplex $\Delta H_m^{100} = 142$ J·g^{-1} normalized by the PLA content in the blend (Table 1).[30] [c] Calculated from the melting enthalpy of PLA stereocomplex and PLA content of the blends as measured by DSC. [d] Actuation performance measured in the shape-memory experiments, as calculated from $\varepsilon_{rev}' = \frac{l_b - l_a}{l_a} \cdot 100\% = \frac{\varepsilon_b - \varepsilon_a}{\varepsilon_a + 100} \cdot 100\%$, where l_a and ε_a are the length of the sample and its engineering strain at the beginning of the actuation cycle at T_{high} and l_b and ε_b are the length of the sample and its engineering strain at the beginning of the actuation cycle at T_{low}.

As the PCL segments provide both the skeleton and the actuator domains, the skeleton / actuator ratio can be varied by modifying the temperature profile of the rbSME process.[7] In contrast to material systems where geometry-determining and actuation domains have different chemistry and structure, the variation of skeleton / actuator ratio in the described PLLA-PCL / PDLA blends can

be performed by modifying T_{high} of a rbSME. To determine the optimum T_{high} an actuation cycle was conducted between $T_{low} = 0$ °C and a T_{high} which was raised between 50 °C and 100 °C in 5 °C increments for each consequent cycle with sample PLLA15-PCL64-SC10. The cycle with the highest ε_{rev}' was used to determine the T_{high} value used in subsequent experiments. The highest value of ε_{rev}', 7.9±0.5%, was measured for the sample PLLA15-PCL64-SC10 at $T_{high} = 55$ °C (Figure S11). As a result, the temperature range for each actuation cycle was set as 0 – 55 °C. The actuation performance of PLLA-PCL / PDLA blend samples was measured over three cycles. The mixed glass transition of the multiblock copolymer was determined by DMTA as $T_g = -40 \pm 3$ °C for all samples. This transition lies outside of the rbSME temperature range and subsequently does not interfere with the actuation performance of our samples.
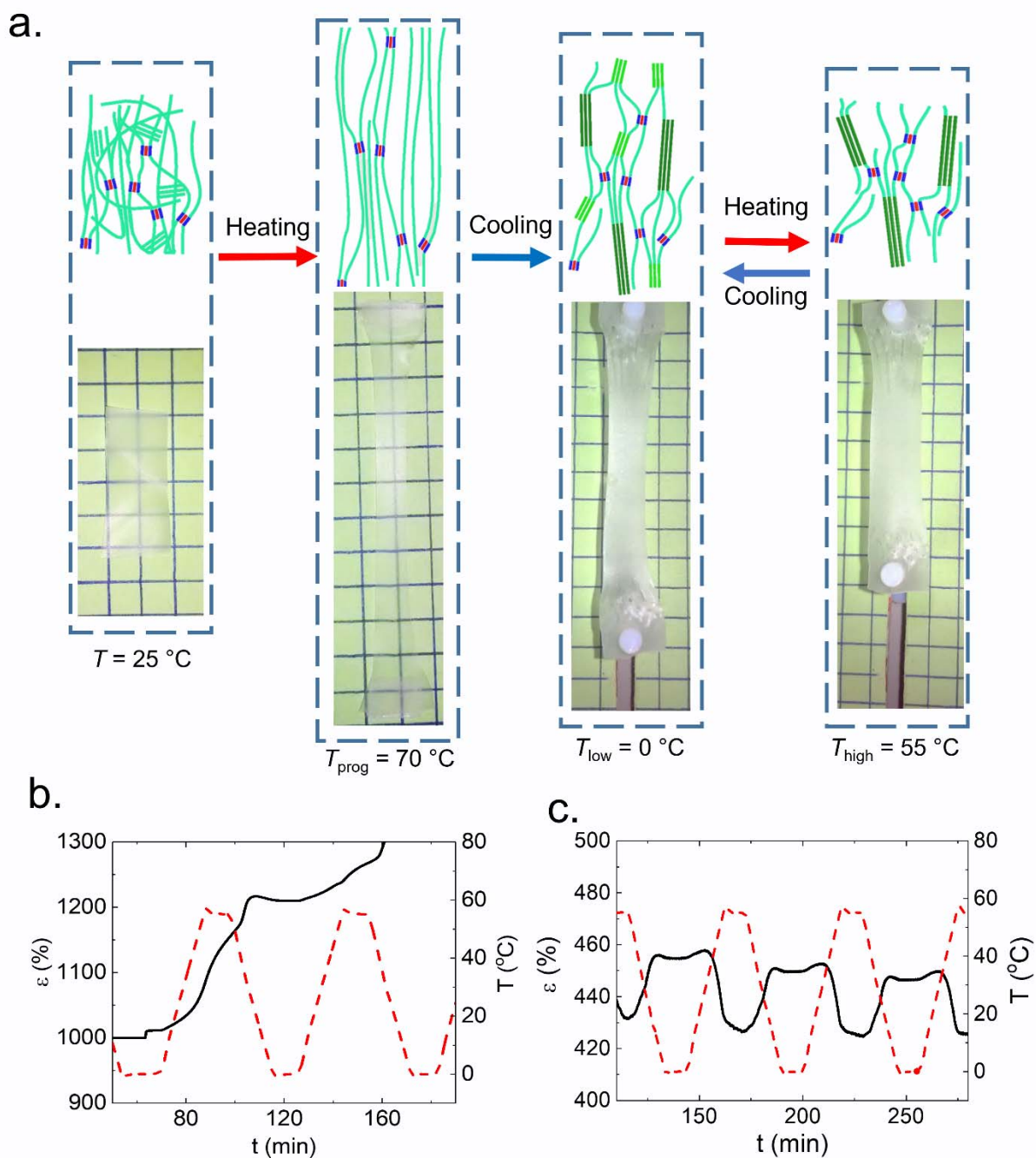
Figure 4. (a) (top) Schematic illustration of structural changes within PLLA-PCL multiblock copolymer blends during actuation. The orientation of the polymer chains is kept by the PCL skeleton domains (dark green) while the network is cross-linked by PLA stereocomplex (blue – PLLA, red – PDLA). Crystallization and melting of the PCL actuator domains (light green) drives the actuation. (a) (bottom) Image series showing shape change of a film sample during programming and actuation with no external stress applied. (b) rbSME curves of PLLA15-PCL64 and (c) PLLA15-PCL64-SC10 as measured by cyclic thermomechanical testing. The black line shows the strain change during the experiment as the sample is exposed to a cyclic temperature change (red dotted line).

PLLA15-PCL64 samples without stereocomplexation show no rbSME (Figure 4b). Without stereocomplex crystallites the material is not able to generate sufficient network anisotropy on deformation. However, samples blended with PDLA (PLLA15-PCL64-SC10) display a sustained actuation performance (Figure 4c), due to the presence of PLA stereocomplex induced cross-linking. The shape transformation of an axially programmed PLLA15-PCL64-SC10 strip during programming and actuation is shown in Figure 4a.

To determine the dependency of $\varepsilon_{rev}{'}$ on the molecular weight of the PDLA homopolymer component of the blends, cyclic thermomechanical testing was performed on blend samples containing PDLA homopolymer with average chain lengths of 3, 6 and 9 repeating units as determined by NMR. Testing revealed that the variation in actuation performance $\varepsilon_{rev}{'}$ with the reduction of PDLA homopolymer average chain length from 26 to 7 repeating units was below the margin of error calculated $\Delta\varepsilon_{rev}{'} = 1.5\%$ for the measurements. However, samples prepared from PDLA homopolymer with an average segment length of 3 showed no actuation capability, consistent with the relatively low stereocomplex crystallinity value, 4±0.4%, obtained in DSC measurements of this sample.

A reduction of PDLA weight content in the blends was observed to lead to an increase of $\varepsilon_{rev}{'}$. With the decrease of PDLA26 in the matrix from 10 wt.% to 1 wt.% the $\varepsilon_{rev}{'}$ increased from $5.9 \pm 0.5\%$ to $12.5 \pm 0.5\%$, where the stereocomplex content was measured using DSC. The observed effect can be understood in comparison with traditional covalently cross-linked rbSME-matrices, where the actuation performance is highly dependant on the cross-link density. If the crosslink density of the network is too high, deformation causes breakage of the intermolecular interactions providing crosslinking before a change in molecular orientation occurs. If the crosslink density is too low, deformation of the material causes slippage of the polymer chains without a corresponding change in molecular orientation. At large number average molecular weights ($M_n >$ 200 kg·mol^{-1}) and a number average molecular weight of the PLLA-PCL diblock repeating unit

of approx. 8 kg·mol^{-1} (average block lengths of 64 hydroxyhexanoate repeating units and 15 *L*-lactide repeating units), a stereocomplex content of 0.8 ± 0.1 wt.% was sufficient to ensure a rbSME.
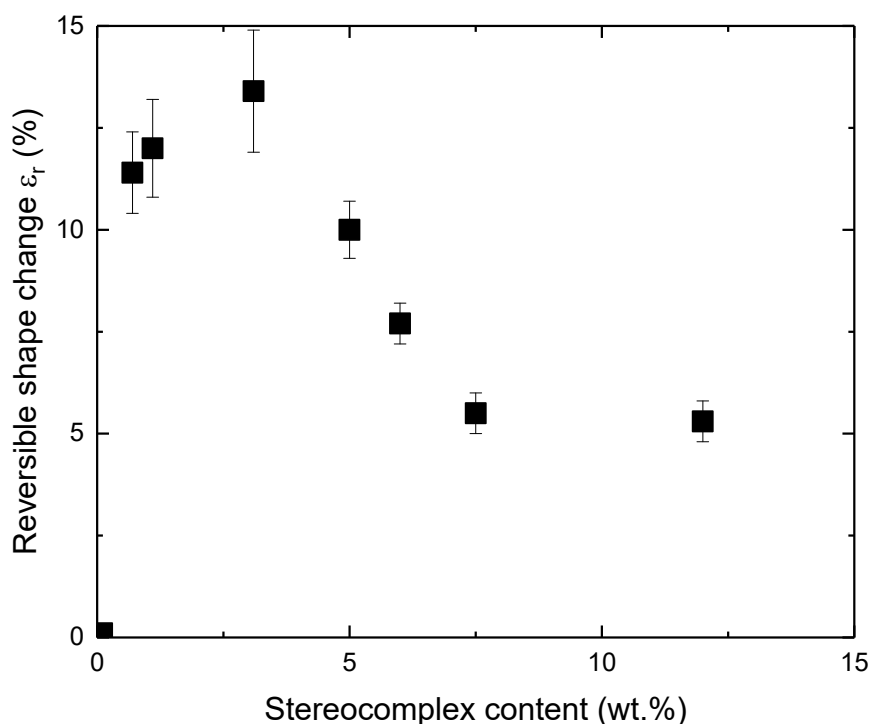
Figure 5. Reversible shape change ($\varepsilon_{\mathrm{rev}}'$) of PLLA-PCL / PDLA blend samples with varying PLA stereocomplex content. $\varepsilon_{\mathrm{rev}}'$ was determined using cyclic thermomechanical testing, stereocomplex content was determined by DSC.

Changing the weight ratio of PLLA-PCL and PDLA in the blends directly leads to the variation of PLA stereocomplex content. The effect of PLA stereocomplex crystallite content, i.e. cross-linking density, on the magnitude of the rbSME in experiments with identical programming parameters ($\varepsilon_0 = 1000\%$, $T_{\mathrm{prog}} = 70\ °C$) is shown in Figure 5. rbSME performance increased with an increase in PLA stereocomplex concentration to a content of 3.1 ± 0.2% wt., after which a drop off of $\varepsilon_{\mathrm{rev}}'$ is observed.

Conclusion

In this paper we demonstrate how the stereocomplexation of a poly(L-lactide) and poly(ε-caprolactone) (PLLA-PCL) multiblock copolymer with a poly(D-lactide) oligomer (PDLA) can be used to provide anchoring points for physical network formation. The ability to introduce physical cross-linking via a blending process enabled the efficient variation of mechanical properties of a shape-memory actuator. Cyclic thermomechanical testing was used to investigate the effect of blend composition on the actuation performance of the material, with a maximum actuation performance of $\varepsilon_{\mathrm{rev}}' = 13.4 \pm 1.5\%$ measured. This method, capable of the realization of such actuation behaviour in a reprocessable material, presents significant advantages over similar shape-changing materials, which are often limited to a single post-processing form. With this work we demonstrate a powerful and efficient method to modify material composition, and subsequent mechanical behavior, without the synthetic modification of polymer architecture. Such methods to adjust the network structure of physically cross-linked materials through *in-situ* processing should provide a platform for the creation of low cost reconfigurable devices in robotics and biomedicine.

Supporting Information

Figure S1. NMR spectra of PLLA15-PCL64 multiblock copolymer

Table S1. Molecular structure of PLLA15-PCL64

Figure S2. Schematic illustrating thermomechanical treatment procedure

Figure S3. Molecular weight distributions of PDLA oligomers

Figure S4 WAXS spectra of blend samples containing PLLA15-PCL64-SC10

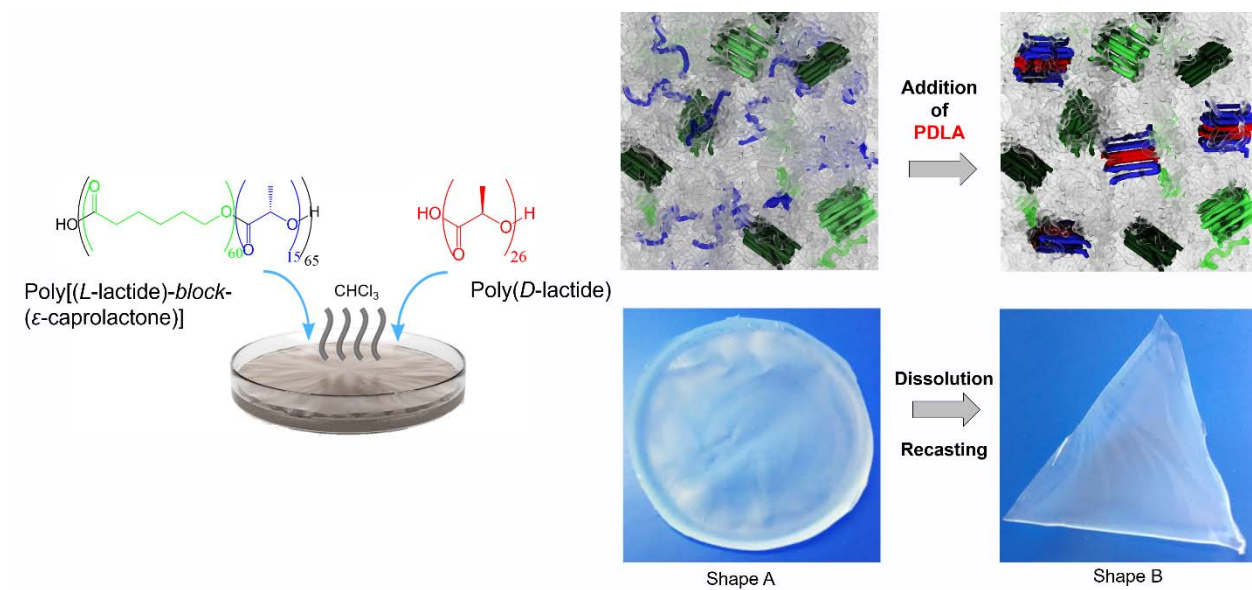**Figure S5** DSC traces of blend samples containing PLLA15-PCL64-SC10

References

1. Yoshida, R.; Uchida, K.; Kaneko, Y.; Sakai, K.; Kikuchi, A.; Sakurai, Y.; Okano, T., Comb-type grafted hydrogels with rapid deswelling response to temperature changes. *Nature* **1995,** 374, 240-242.
2. Yuk, H.; Lin, S.; Ma, C.; Takaffoli, M.; Fang, N. X.; Zhao, X., Hydraulic hydrogel actuators and robots optically and sonically camouflaged in water. *Nat. Commun.* **2017,** 8, 1-12.
3. Yew, Y. K.; Ng, T. Y.; Li, H.; Lam, K. Y., Analysis of pH and electrically controlled swelling of hydrogel-based micro-sensors/actuators. *Biomed. Microdevices* **2007,** 9, 487-499.
4. Lagerwall, J. P. F.; Scalia, G., A new era for liquid crystal research: Applications of liquid crystals in soft matter nano-, bio- and microtechnology. *Curr. Appl. Phys.* **2012,** 12, 1387-1412.
5. Yu, H.; Ikeda, T., Photocontrollable liquid-crystalline actuators. *Adv. Mater.* **2011,** 23, 2149-2180.
6. Kularatne, R. S.; Kim, H.; Boothby, J. M.; Ware, T. H., Liquid crystal elastomer actuators: Synthesis, alignment, and applications. *J. Polym. Sci., Part B: Polym. Phys.* **2017,** 55, 395-411.
7. Behl, M.; Kratz, K.; Zotzmann, J.; Nöchel, U.; Lendlein, A., Reversible bidirectional shape-memory polymers. *Adv. Mater.* **2013,** 25, 4466-9.
8. Lendlein, A., Fabrication of reprogrammable shape-memory polymer actuators for robotics. *Sci. Robot.* **2018,** 3, (18), eaat9090.
9. Zhao, Q.; Qi, H. J.; Xie, T., Recent progress in shape memory polymer: New behavior, enabling materials, and mechanistic understanding. *Prog. Polym. Sci.* **2015,** 49-50, 79-120.
10. Hu, J.; Zhu, Y.; Huang, H.; Lu, J., Recent advances in shape-memory polymers: Structure, mechanism, functionality, modeling and applications. *Prog. Polym. Sci.* **2012,** 37, 1720-1763.
11. Lendlein, A.; Gould, O. E. C., Reprogrammable recovery and actuation behaviour of shape-memory polymers. *Nat. Rev. Mater.* **2019,** 4, 116-133.
12. Guo, Q.; Bishop, C. J.; Meyer, R. A.; Wilson, D. R.; Olasov, L.; Schlesinger, D. E.; Mather, P. T.; Spicer, J. B.; Elisseeff, J. H.; Green, J. J., Entanglement-Based Thermoplastic Shape Memory Polymeric Particles with Photothermal Actuation for Biomedical Applications. *ACS Appl. Mater. Interfaces* **2018,** 10, 13333-13341.
13. Gu, X.; Mather, P. T., Entanglement-based shape memory polyurethanes: Synthesis and characterization. *Polymer* **2012,** 53, 5924-5934.
14. Zhou, S.; Zheng, X.; Yu, X.; Wang, J.; Weng, J.; Li, X.; Feng, B.; Yin, M., Hydrogen bonding interaction of poly(D,L-lactide)/hydroxyapatite nanocomposites. *Chem. Mater.* **2007,** 19, 247-253.
15. Yan, W.; Rudolph, T.; Noechel, U.; Gould, O.; Behl, M.; Kratz, K.; Lendlein, A., Reversible Actuation of Thermoplastic Multiblock Copolymers with Overlapping Thermal Transitions of Crystalline and Glassy Domains. *Macromolecules* **2018,** 51, (12), 4624-4632.
16. Dolog, R.; Weiss, R. A., Shape memory behavior of a polyethylene-based carboxylate ionomer. *Macromolecules* **2013,** 46, 7845-7852.
17. Lu, L.; Li, G., One-Way Multishape-Memory Effect and Tunable Two-Way Shape Memory Effect of Ionomer Poly(ethylene-co-methacrylic acid). *ACS Appl. Mater. Interfaces* **2016,** 8, 14812-14823.
18. Gao, Y.; Liu, W.; Zhu, S., Polyolefin Thermoplastics for Multiple Shape and Reversible Shape Memory. *ACS Appl. Mater. Interfaces* **2017,** 9, (5), 4882-4889.
19. Farhan, M.; Rudolph, T.; Nöchel, U.; Kratz, K.; Lendlein, A., Extractable free polymer chains enhance actuation performance of crystallizable poly(ε-caprolactone) networks and enable self-healing. *Polymers* **2018,** 10, (3), 255.
20. Kolesov, I.; Dolynchuk, O.; Borreck, S., Morphology-controlled multiple one- and two-way shape-memory behavior of cross-linked polyethylene / poly(ε -caprolactone) blends. *Polym. Adv. Technol.* **2014,** 25, (11), 1315-1322.
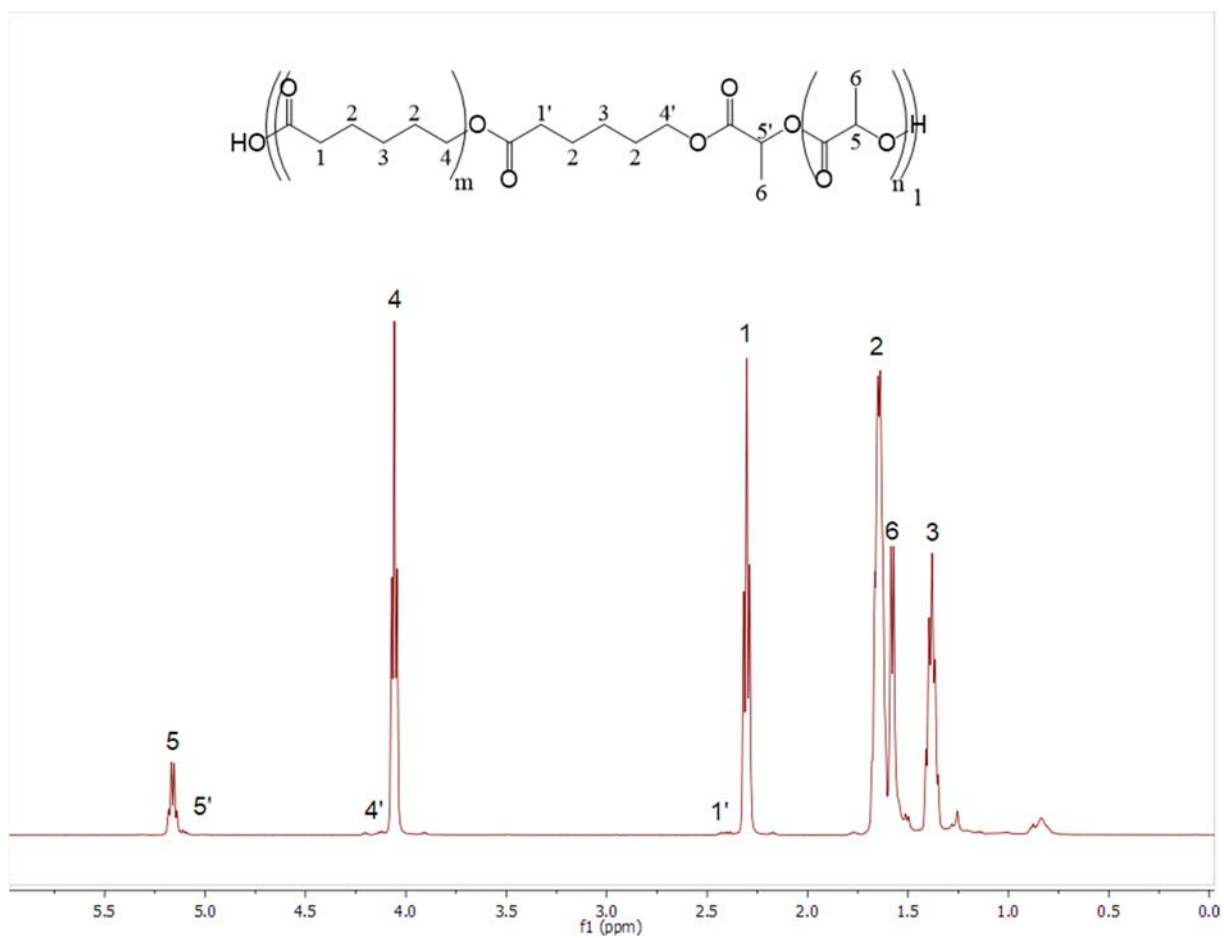
21. Tsuji, H.; Ikada, Y., Stereocomplex formation between enantiomeric poly (lactic acids). 9. Stereocomplexation from the melt. *Macromolecules* **1993,** 26, 6918-6926.

22. Tsuji, H., Poly(lactic acid) stereocomplexes: A decade of progress. *Adv. Drug Del. Rev.* **2016,** 107, 97-135.

23. Yang, D. D.; Liu, W.; Zhu, H. M.; Wu, G.; Chen, S. C.; Wang, X. L.; Wang, Y. Z., Toward Super-Tough Poly(l-lactide) via Constructing Pseudo-Cross-link Network in Toughening Phase Anchored by Stereocomplex Crystallites at the Interface. *ACS Appl. Mater. Interfaces* **2018,** 10, (31), 26594-26603.

24. de Jong, S. J.; van Dijk-Wolthuis, W. N. E. E.; Kettenes-Van Den Bosch, J. J.; Schuyl, P. J. W. W.; Hennink, W. E., Monodisperse Enantiomeric Lactic Acid Oligomers: Preparation, Characterization, and Stereocomplex Formation. *Macromolecules* **1998,** 31, 6397-6402.

25. Loo, Y. L.; Register, R. A.; Ryan, A. J., Polymer crystallization in 25-nm spheres. *Phys. Rev. Lett.* **2000,** 84, (18), 4120-3.

26. Huang, P.; Zhu, L.; Cheng, S. Z. D.; Ge, Q.; Quirk, R. P.; Thomas, E. L.; Lotz, B.; Hsiao, B. S.; Liu, L.; Yeh, F., Crystal Orientation Changes in Two-Dimensionally Confined Nanocylinders in a Poly(ethylene oxide)-b-polystyrene/Polystyrene Blend. *Macromolecules* **2001,** 34, (19), 6649-6657.

27. Lendlein, A.; Neuenschwander, P.; Suter, U. W., Hydroxy-telechelic copolyesters with well defined sequence structure through ring-opening polymerization. *Macromol. Chem. Phys.* **2000,** 201, (11), 1067-1076.

28. Jikei, M.; Suga, T.; Yamadoi, Y.; Matsumoto, K., Synthesis and properties of poly(L-lactide-co-glycolide)-b-Poly(ϵ-caprolactone) multiblock copolymers formed by self-polycondensation of diblock macromonomers. *Polym. J.* **2017,** 49, 369-375.

29. Jikei, M.; Takeyama, Y.; Yamadoi, Y.; Shinbo, N.; Matsumoto, K.; Motokawa, M.; Ishibashi, K.; Yamamoto, F., Synthesis and properties of Poly(L-lactide)-Poly(ε-caprolactone) multiblock copolymers by the self-polycondensation of diblock macromonomers. *Polym. J.* **2015,** 47, 657-665.

30. Jikei, M.; Yamadoi, Y.; Suga, T.; Matsumoto, K., Stereocomplex formation of poly(L-lactide)-poly(ε-caprolactone) multiblock copolymers with Poly(D-lactide). *Polymer* **2017,** 123, 73-80.

31. Moore, J. S.; Stupp, S. I., Room temperature polyesterification. *Macromolecules* **1990,** 23, 65-70.

32. Perego, G.; Vercellio, T.; Balbontin, G., Copolymers of L- and D,L-lactide with 6-caprolactone: synthesis and characterization. *Die Makromolekulare Chemie* **1993,** 194, 2463-2469.

33. Crescenzi, V.; Manzini, G.; Calzolari, G.; Borri, C., Thermodynamics of fusion of poly-β-propiolactone and poly-ε\{lunate\}-caprolactone. comparative analysis of the melting of aliphatic polylactone and polyester chains. *Eur. Polym. J.* **1972,** 8, 449-463.

34. Tsuji, H., Poly(lactide) Stereocomplexes: Formation, Structure, Properties, Degradation, and Applications. *Macromol. Biosci.* **2005,** 5, (7), 569-597.

35. Hiss, R.; Hobeika, S.; Lynn, C.; Strobl, G., Network Stretching, Slip Processes, and Fragmentation of Crystallites during Uniaxial Drawing of Polyethylene and Related Copolymers. A Comparative Study. *Macromolecules* **1999,** 32, 4390-4403.

36. Hong, K.; Rastogi, A.; Strobl, G., A model treating tensile deformation of semicrystalline polymers: Quasi-static stress-strain relationship and viscous stress determined for a sample of polyethylene. *Macromolecules* **2004,** 37, 10165-10173.

For table of contents only

Poly[(L-lactide)-block-(ε-caprolactone)]   CHCl$_3$ Poly(D-lactide)

Addition of **PDLA**

Dissolution

Recasting

Shape A   Shape B

Supporting information

Figure S1. 500 MHz ^{1}H NMR spectra of PLLA15-PCL64 measured in CDCl$_3$ solution.

Table S1. Molecular structure of the reported PLLA-PLC and their precursors.

Sample[a]	M_{NMR}[b], kg·mol^{-1}	M_n[c], kg·mol^{-1}	M_w[c], kg·mol^{-1}	Đ[c]	PLA/ PCL[d]	PCL block length, repeat units[e]	PLA block length, repeat units[e]
PCL64	9.7	12	20	1.6	-	85	-
PLLA15-PCL64 diblock precursor	12.2	17	25	1.48	16/84	65	27
PLLA15-PCL64	-	238	483	2.03	17/83	64	15

[a] The sample name PLLAX-PCLY, where X indicates the PLLA average block length of the end product PLLA-PCL multiblock copolymer determined with ^{1}H‾NMR and Y indicates the PCL number average block length of the end product PLLA-PCL multiblock copolymer determined with ^{1}H‾NMR.

[b] Determined with ^{1}H‾NMR as ratio of the integral intensity of a quadruplet in the 5.2 region attributed to CH-signal of a chain unit of PLLA segments and a quadruplet in the 4 ppm region attributed to PCL CH_2-signal of a chain unit (Figure S1) to the integral intensity of a quadruplet in 4.4 ppm region attributed to PLLA carboxyl end group for the block copolymer samples and a quadruplet in 3.8 ppm region attributed to PCL carboxyl end group for the PCL homopolymer. The ratios were then multiplied by the molecular weight M_{PLA} = 72 kg · mol^{-1} and M_{PCL} = 114 kg · mol^{-1} respectively.

[c] Number and weight-average molecular weight and polydispersity index. Determined with a multidetector GPC setup against universal calibration using tetrahydrofuran as eluent with a flow rate of 1 mL · min^{-1} equipped with a light scattering detector. Where Đ was calculated as a ratio of weight and number average molecular weight.

[d] Calculated from ^{1}H‾NMR spectra as the ratio of the integral intensities of a quadruplet in the 5.2 region attributed to CH-signal of a chain unit of PLLA segments and a quadruplet in the 4 ppm region attributed to PCL CH_2-signal of a chain unit (Figure S1).

[e] Determined with ^{1}H‾NMR as a ratio of the integral intensities (quadruplet in the 5.2 region attributed to CH-signal of a chain unit of PLLA segments and a quadruplet in the 4 ppm region attributed to PCL CH_2-signal of a chain unit (Figure S1)) of the main peak and its right or left shoulder for PLLA and PCL respectively. Where the main peak is attributed to the repeating units having the same neighbor and the shoulder having the same multiplicity is attributed to the repeating units having a different neighbor in the multiblock copolymer chain.

The error of GPC was considered as 10% of the measured value according to deviations in the calibration curve achieved for the machine with polystyrene standards.

The deviation of ^{1}H‾NMR data was considered as combination of saturation effects, unevenness of the magnetic field in the sample and the line shape causing overlapping of the peaks. The last element has the highest input into the calculation error resulting total deviation of approx. 12%.
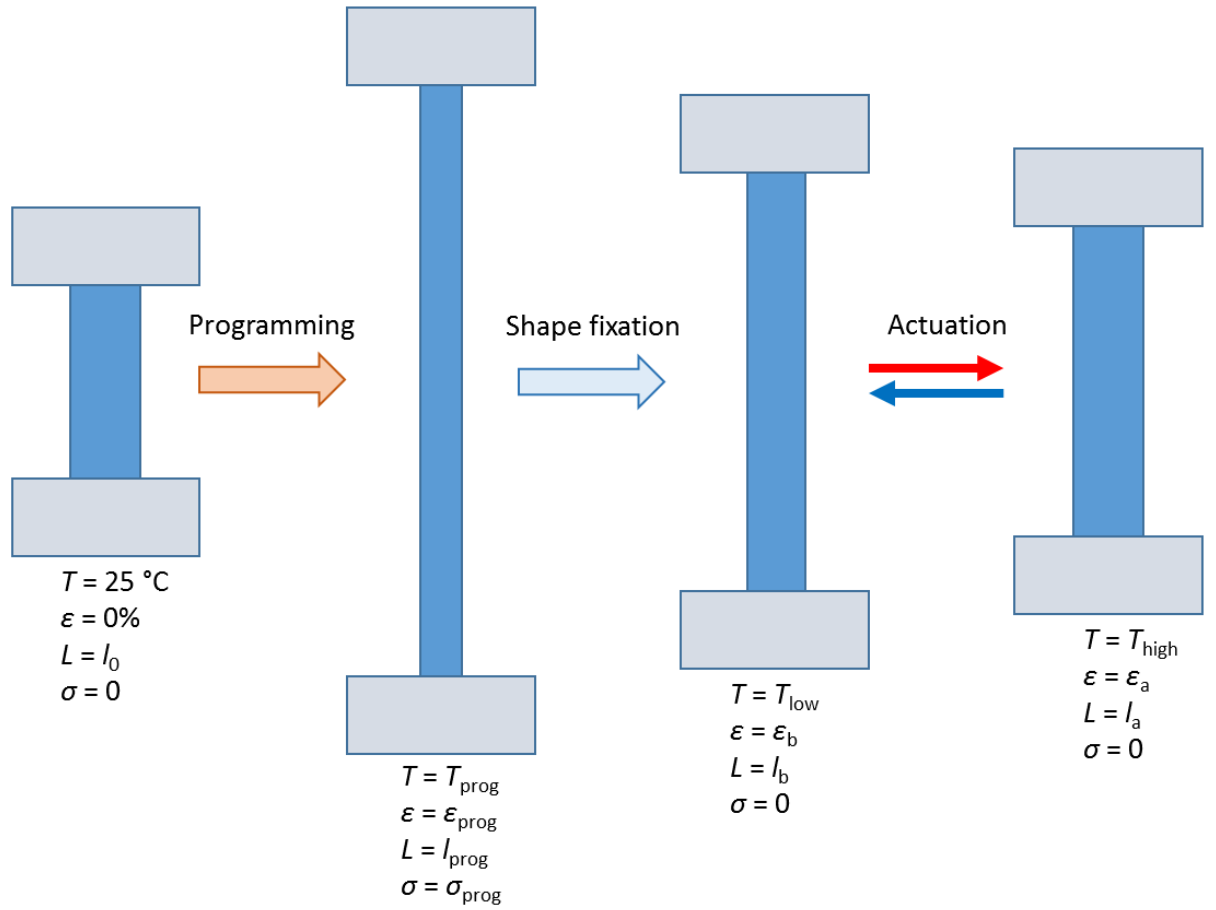
Figure S2. Schematic illustration of thermomechanical treatment in rbSME experiments. A dog-bone shaped sample is fixed in a tensile testing machine in an undeformed (no strain ε applied to the sample and its length $L = l_0$) not loaded state ($\sigma_0 = 0$) at the room temperature $T = 25$ °C. The sample is programmed by deformation at T_{prog} to the programming strain ε_{prog}. In the following step the shape is fixed by cooling the sample to T_{low} before reduction of the applied stress σ to 0. The actuation cycle is performed by subsequent changing the temperature in the thermo chamber of the tensile machine between T_{low} and T_{high}, which causes changes in sample length due to crystallization-induced elongation and melting-induced contraction.
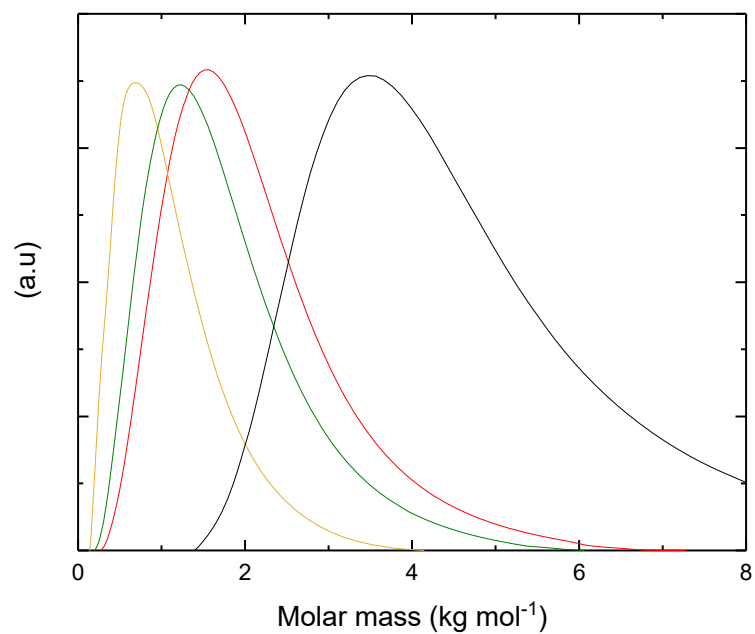
Figure S3. Molecular weight distributions of PDLA oligomers PDLA3 (yellow), PDLA6 (green), PDLA9 (red) and PDLA26 (black). Measurements were performed on a multidetector GPC setup against universal calibration in THF and an eluent flow rate of 1 mL·min^{-1}.
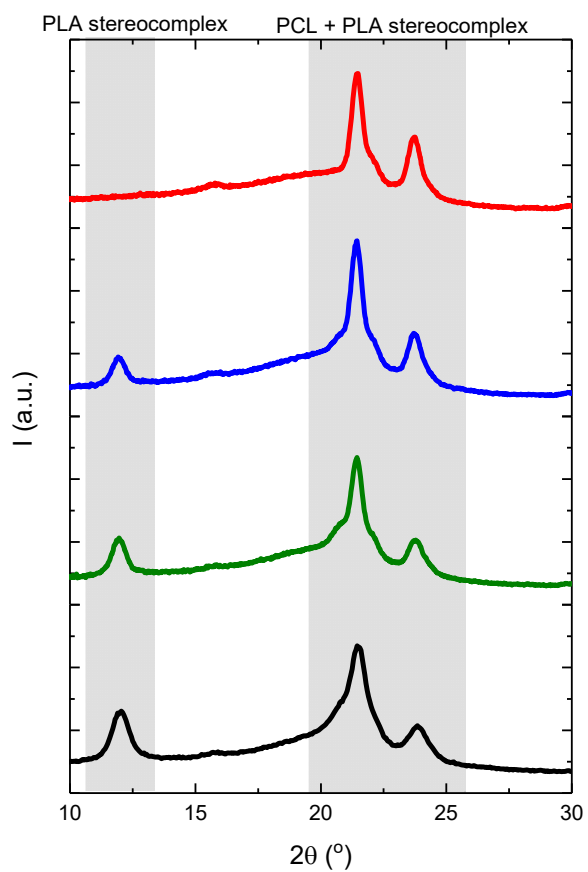
Figure S4. WAXS spectra at the ambient temperature of blend samples containing PLLA15-PCL64-SC10 multiblock copolymer with PDLA homopolymers of different number average lengths: 3 (red), 6 (blue), 9 (green) and 26 (black) repeating units determined with ^{1}H NMR.
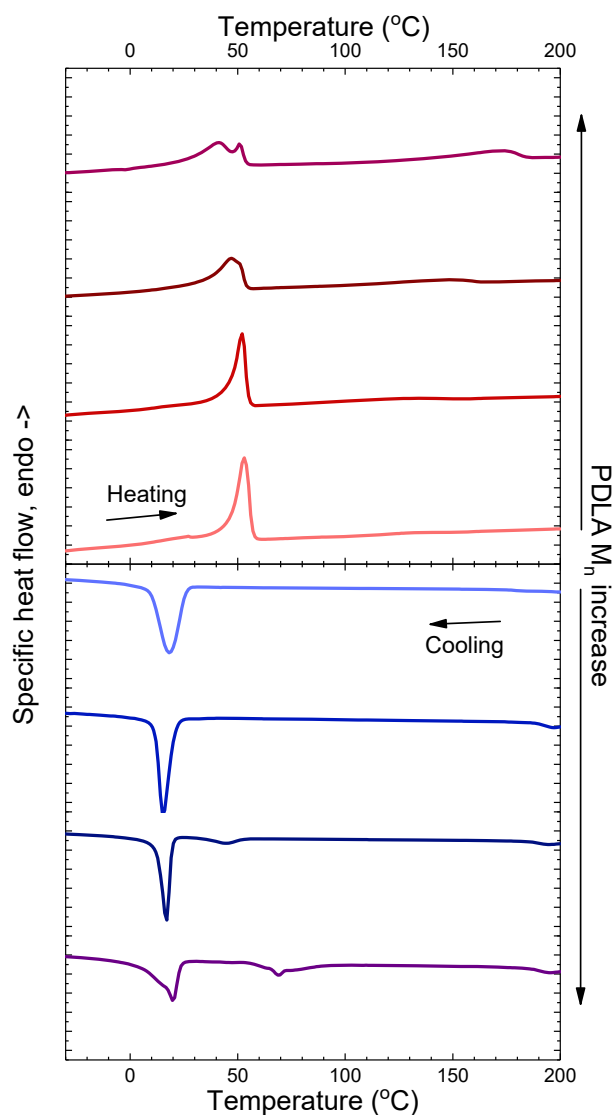
Figure S5. DSC traces of blend samples containing PLLA15-PCL64-SC10 multiblock copolymer with PDLA homopolymers of different number average lengths in order starting from the central x-axis: 3, 6, 9 and 26 repeating units determined with ^{1}H NMR. The second heating (red curves) and the first cooling (blue curves) runs at 10 °C heating/cooling rate.

Table S2. Average molecular weight and polydispersity of PDLA homopolymers.

Sample[a]	Segment length, repeating units[b]	M_n, kg · mol^{-1} [c]	M_w, kg · mol^{-1} [c]	Đ[c]
PDLA3	3	0.6	0.8	1.42
PDLA6	6	1	1.4	1.35
PDLA9	9	1.3	1.7	1.31
PDLA26	26	3.5	4.1	1.17

[a] The sample name PDLAX where X indicates the PDLA segment length determined with ^{1}H-NMR. [b] Determined with ^{1}H-NMR as ratio of the integral intensity of a quadruplet in the 5.2 region attributed to CH-signal of a chain unit of PDLA and a quadruplet in the 4.4 ppm region attributed to PLLA carboxyl end group. [c] Number and weight-average molecular weight and polydispersity index. Determined with GPC against universal calibration using tetrahydrofuran as eluent with a flow rate of 1 mL · min^{-1} equipped with a light scattering detector. Where Đ was calculated as a ratio of weight and number average molecular weight.
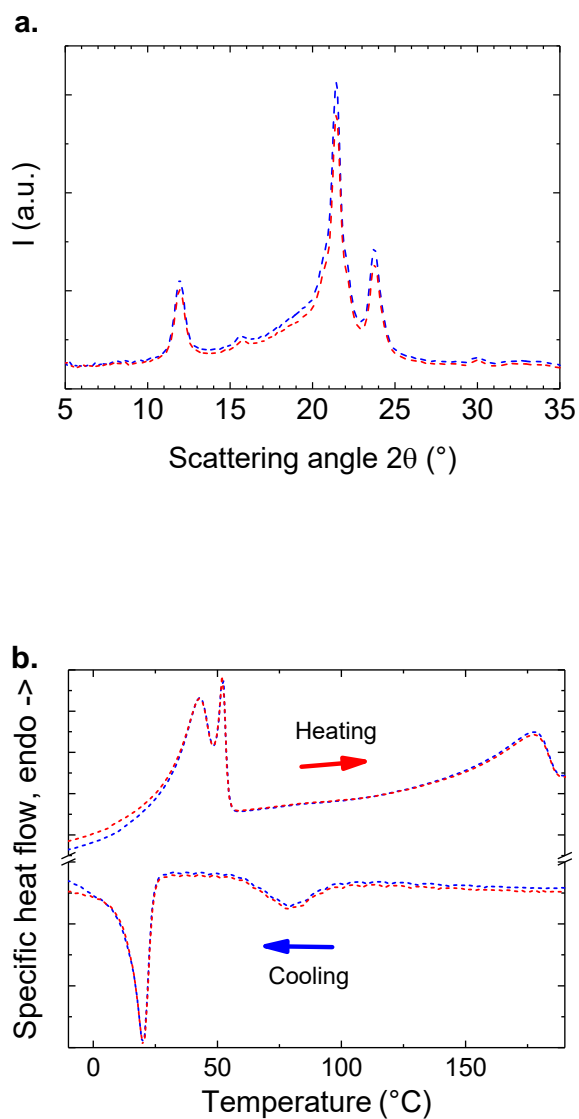
Figure S6. (a) WAXS spectra and (b) DSC traces of PLLA15-PCL64-SC10 initial sample (blue) and re-casted physical network (red), here the second heating and first cooling traces with 10 °C min^{-1} rates are shown.
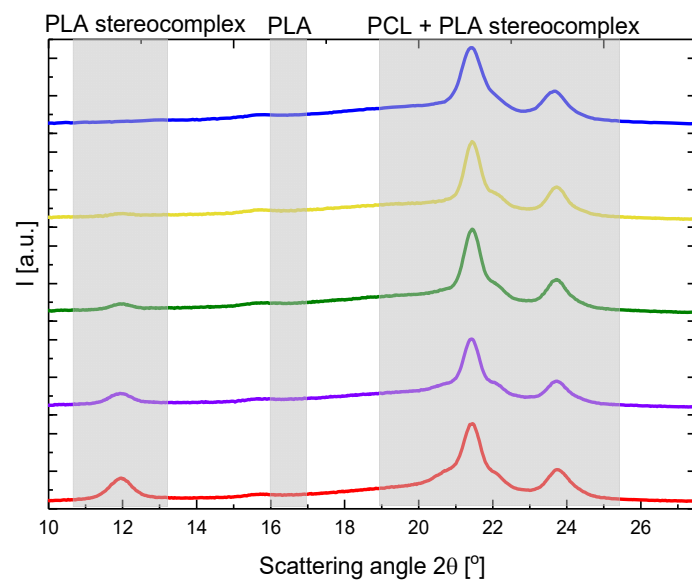
Figure S7. WAXS spectra of PLLA12-PCL58 (blue), PLLA15-PCL64-SC1 (yellow), PLLA15-PCL64-SC2 (green), PLLA15-PCL64-SC5 (purple) and PLLA15-PCL64-SC10 (red) at 25 °C
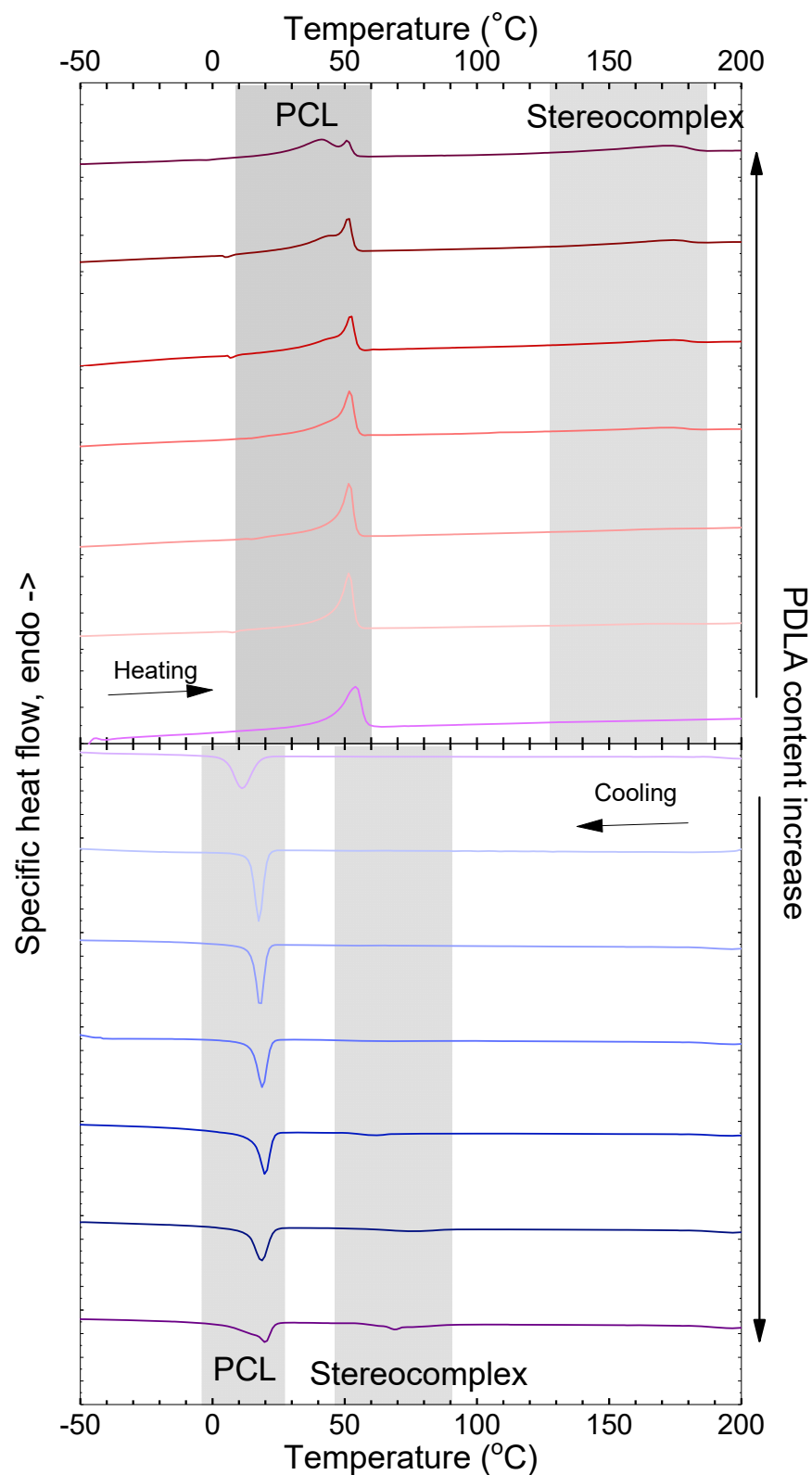
Figure S8. DSC traces of PLLA-PCL / PDLA blends with different PDLA content in order starting from the central x-axis: PLLA15-PCL64, PLLA15-PCL64-SC1, PLLA15-PCL64-SC2, PLLA15-PCL64-SC3, PLLA15-PCL64-SC4, PLLA15-PCL64-SC5, PLLA15-PCL64-SC10. The second heating and the first cooling runs at 10 °C heating/cooling rate.
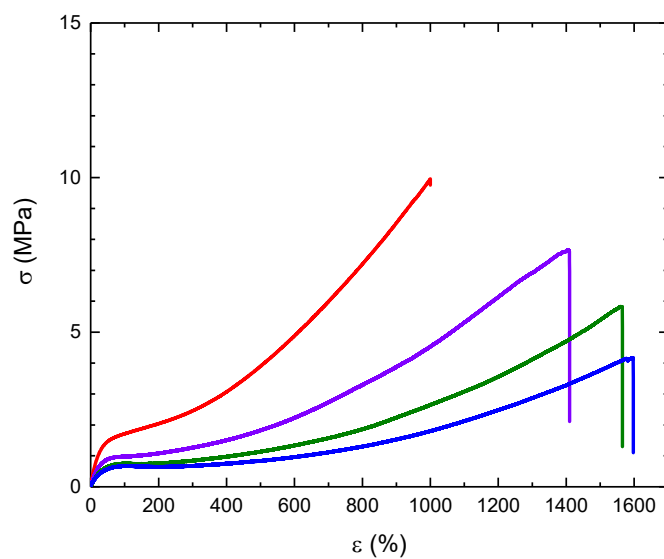
Figure S9. Stress-strain curves at 70 °C and deformation rate 5 mm min^{-1} of PLLA15-PCL64 blended with different amounts of PDLA. Blue – PLLA15-PCL64-SC01, green – PLLA15-PCL64-SC02, purple PLLA15-PCL64-SC05, red – PLLA15-PCL64-SC10
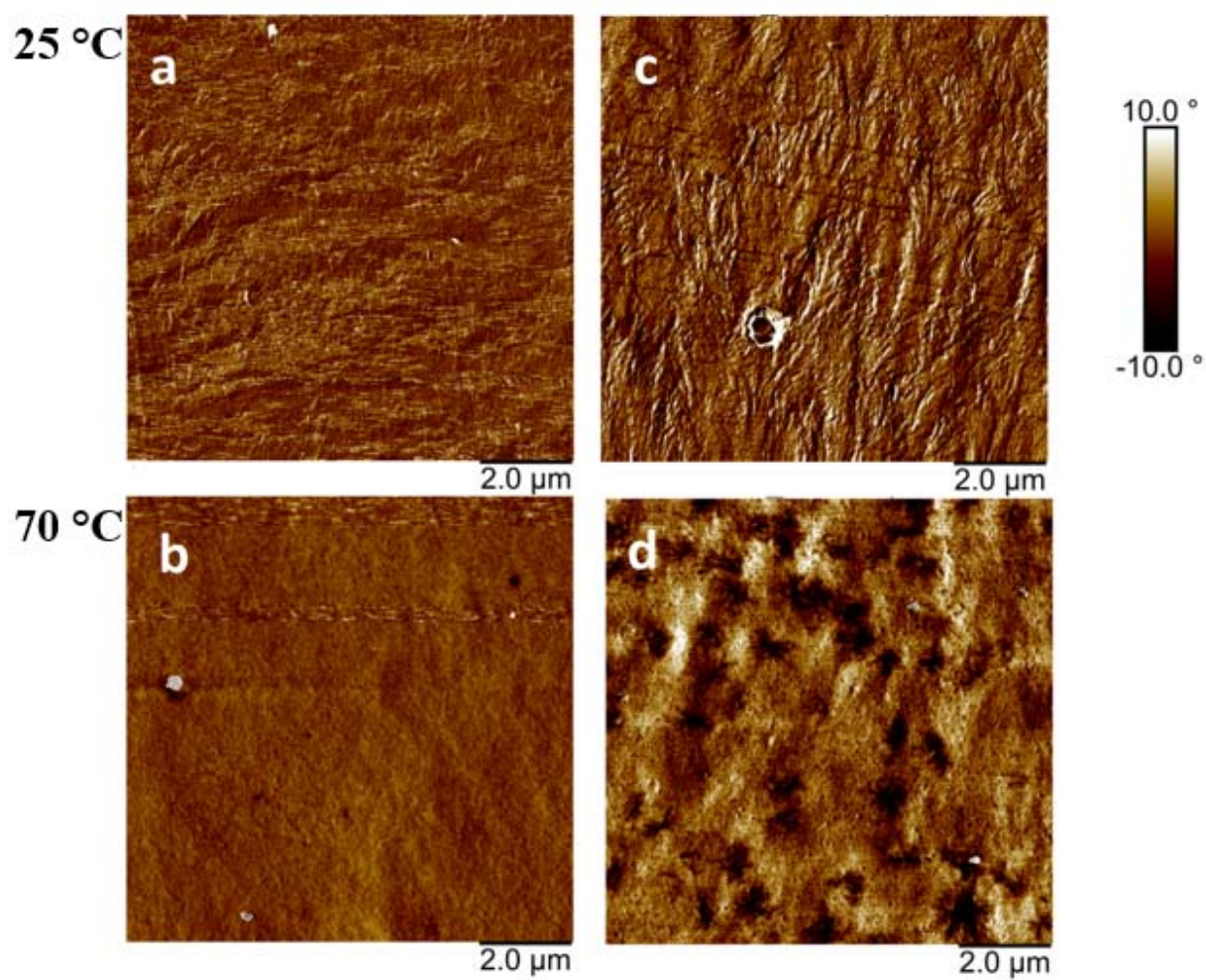
Figure S10. AFM phase image of PLLA-PCL multiblock copolymer at 25 °C (a) and 70 °C (b) and its blend with 10 wt.% of PDLA at 25 °C (c) and 70 °C (d)

Table S3. Effect of the programming strain ε_{prog}, on the actuation performance $\varepsilon_{rev}{}'$ of PLLA-PCL / PDLA blends.

Sample name[a]	ε_{prog}, %[b]	$\varepsilon_{rev}{}'$, %[c]
PLLA15-PCL64-SC10	750	5.3±0.5
	1000	5.3±0.5
PLLA15-PCL64-SC5	500	8.9±1.2
	750	6.1±0.5
	1000	7.7±0.5
PLLA15-PCL64-SC2	500	10±1.5
	750	10±0.9
	1000	12±1.2
PLLA15-PCL64-SC1	500	12.6±1.5
	750	11.8±1.3
	1000	11.4±1.5
	1250	11±1.5

[a] The sample name LLAX-CLY-SCZ, where X and Y indicate the block length of PLLA and PCL respectively determined with ^{1}H-NMR, and Z indicates, the weight content of PDLA in the blend. [b] Programming elongation of the rbSME experiment. [c] Reversible actuation performance determined as the ratio of the change in the sample length in an actuation cycle to its length in the beginning of the cycle at T_{high}
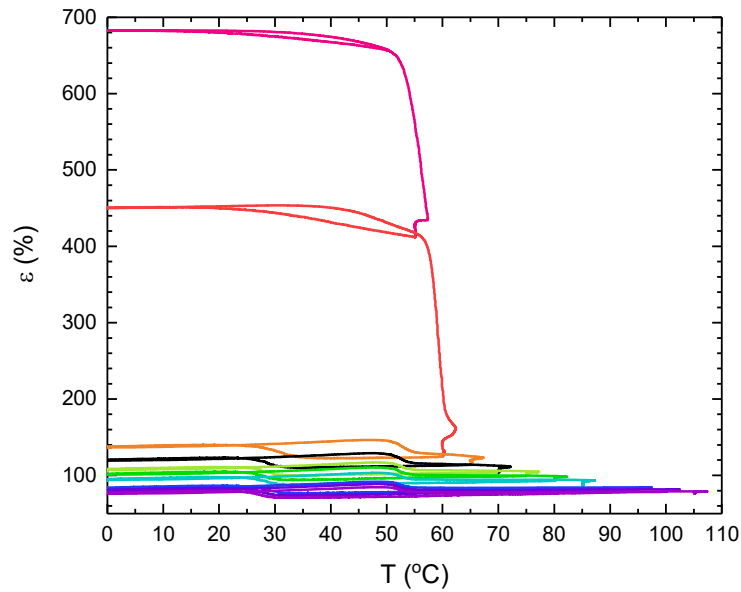
Figure S11. Reversible elongation change of PLLA15-PCL64-SC10 with a variation of T_{high}, as measured by cyclic thermomechanical testing.